International Journal of Physical Sciences

October 2013 - Vol. 8 Num. 41

Submit manuscripts: www.ms.academicjournals.org

Editorial Office: ijps@academicjournals.org

URL: www.academicjournals.org

academicJournals

ABOUT IJPS

The **International Journal of Physical Sciences (IJPS)** is published weekly (one volume per year) by Academic Journals.

International Journal of Physical Sciences (IJPS) is an open access journal that publishes high-quality solicited and unsolicited articles, in English, in all Physics and chemistry including artificial intelligence, neural processing, nuclear and particle physics, geophysics, physics in medicine and biology, plasma physics, semiconductor science and technology, wireless and optical communications, materials science, energy and fuels, environmental science and technology, combinatorial chemistry, natural products, molecular therapeutics, geochemistry, cement and concrete research, metallurgy, crystallography and computer-aided materials design. All articles published in IJPS are peer-reviewed.

Submission of Manuscript

Submit manuscripts as e-mail attachment to the Editorial Office at: ijps@academicjournals.org. A manuscript number will be mailed to the corresponding author shortly after submission.

For all other correspondence that cannot be sent by e-mail, please contact the editorial office (at ijps@academicjournals.org).

The International Journal of Physical Sciences will only accept manuscripts submitted as e-mail attachments.

Please read the **Instructions for Authors** before submitting your manuscript. The manuscript files should be given the last name of the first author.

Editorial Board

Instructions for Author

Electronic submission of manuscripts is strongly encouraged, provided that the text, tables, and figures are included in a single Microsoft Word file (preferably in Arial font).

The **cover letter** should include the corresponding author's full address and telephone/fax numbers and should be in an e-mail message sent to the Editor, with the file, whose name should begin with the first author's surname, as an attachment.

Article Types

Three types of manuscripts may be submitted:

Regular articles: These should describe new and carefully confirmed findings, and experimental procedures should be given in sufficient detail for others to verify the work. The length of a full paper should be the minimum required to describe and interpret the work clearly.

Short Communications: A Short Communication is suitable for recording the results of complete small investigations or giving details of new models or hypotheses, innovative methods, techniques or apparatus. The style of main sections need not conform to that of full-length papers. Short communications are 2 to 4 printed pages (about 6 to 12 manuscript pages) in length.

Reviews: Submissions of reviews and perspectives covering topics of current interest are welcome and encouraged. Reviews should be concise and no longer than 4-6 printed pages (about 12 to 18 manuscript pages). Reviews are also peer-reviewed.

Review Process

All manuscripts are reviewed by an editor and members of the Editorial Board or qualified outside reviewers. Authors cannot nominate reviewers. Only reviewers randomly selected from our database with specialization in the subject area will be contacted to evaluate the manuscripts. The process will be blind review.

Decisions will be made as rapidly as possible, and the journal strives to return reviewers' comments to authors as fast as possible. The editorial board will re-review manuscripts that are accepted pending revision. It is the goal of the IJPS to publish manuscripts within weeks after submission.

Regular articles

All portions of the manuscript must be typed double-spaced and all pages numbered starting from the title page.

The Title should be a brief phrase describing the contents of the paper. The Title Page should include the authors' full names and affiliations, the name of the corresponding author along with phone, fax and E-mail information. Present addresses of authors should appear as a footnote.

The Abstract should be informative and completely self-explanatory, briefly present the topic, state the scope of the experiments, indicate significant data, and point out major findings and conclusions. The Abstract should be 100 to 200 words in length.. Complete sentences, active verbs, and the third person should be used, and the abstract should be written in the past tense. Standard nomenclature should be used and abbreviations should be avoided. No literature should be cited.

Following the abstract, about 3 to 10 key words that will provide indexing references should be listed.

A list of non-standard **Abbreviations** should be added. In general, non-standard abbreviations should be used only when the full term is very long and used often. Each abbreviation should be spelled out and introduced in parentheses the first time it is used in the text. Only recommended SI units should be used. Authors should use the solidus presentation (mg/ml). Standard abbreviations (such as ATP and DNA) need not be defined.

The Introduction should provide a clear statement of the problem, the relevant literature on the subject, and the proposed approach or solution. It should be understandable to colleagues from a broad range of scientific disciplines.

Materials and methods should be complete enough to allow experiments to be reproduced. However, only truly new procedures should be described in detail; previously published procedures should be cited, and important modifications of published procedures should be mentioned briefly. Capitalize trade names and include the manufacturer's name and address. Subheadings should be used. Methods in general use need not be described in detail.

Results should be presented with clarity and precision. The results should be written in the past tense when describing findings in the authors' experiments. Previously published findings should be written in the present tense. Results should be explained, but largely without referring to the literature. Discussion, speculation and detailed interpretation of data should not be included in the Results but should be put into the Discussion section.

The Discussion should interpret the findings in view of the results obtained in this and in past studies on this topic. State the conclusions in a few sentences at the end of the paper. The Results and Discussion sections can include subheadings, and when appropriate, both sections can be combined.

The Acknowledgments of people, grants, funds, etc should be brief.

Tables should be kept to a minimum and be designed to be as simple as possible. Tables are to be typed double-spaced throughout, including headings and footnotes. Each table should be on a separate page, numbered consecutively in Arabic numerals and supplied with a heading and a legend. Tables should be self-explanatory without reference to the text. The details of the methods used in the experiments should preferably be described in the legend instead of in the text. The same data should not be presented in both table and graph form or repeated in the text.

Figure legends should be typed in numerical order on a separate sheet. Graphics should be prepared using applications capable of generating high resolution GIF, TIFF, JPEG or Powerpoint before pasting in the Microsoft Word manuscript file. Tables should be prepared in Microsoft Word. Use Arabic numerals to designate figures and upper case letters for their parts (Figure 1). Begin each legend with a title and include sufficient description so that the figure is understandable without reading the text of the manuscript. Information given in legends should not be repeated in the text.

References: In the text, a reference identified by means of an author‘s name should be followed by the date of the reference in parentheses. When there are more than two authors, only the first author‘s name should be mentioned, followed by ’et al‘. In the event that an author cited has had two or more works published during the same year, the reference, both in the text and in the reference list, should be identified by a lower case letter like ’a‘ and ’b‘ after the date to distinguish the works.

Examples:

Abayomi (2000), Agindotan et al. (2003), (Kelebeni, 1983), (Usman and Smith, 1992), (Chege, 1998; 1987a,b; Tijani, 1993,1995), (Kumasi et al., 2001)

References should be listed at the end of the paper in alphabetical order. Articles in preparation or articles submitted for publication, unpublished observations, personal communications, etc. should not be included in the reference list but should only be mentioned in the article text (e.g., A. Kingori, University of Nairobi, Kenya, personal communication). Journal names are abbreviated according to Chemical Abstracts. Authors are fully responsible for the accuracy of the references.

Examples:

Ogunseitan OA (1998). Protein method for investigating mercuric reductase gene expression in aquatic environments. Appl. Environ. Microbiol. 64:695-702.

Gueye M, Ndoye I, Dianda M, Danso SKA, Dreyfus B (1997). Active N2 fixation in several Faidherbia albida provenances. Ar. Soil Res. Rehabil. 11:63-70.

Charnley AK (1992). Mechanisms of fungal pathogenesis in insects with particular reference to locusts. In: Lomer CJ, Prior C (eds) Biological Controls of Locusts and Grasshoppers: Proceedings of an international workshop held at Cotonou, Benin. Oxford: CAB International, pp 181-190.

Mundree SG, Farrant JM (2000). Some physiological and molecular insights into the mechanisms of desiccation tolerance in the resurrection plant Xerophyta viscasa Baker. In Cherry et al. (eds) Plant tolerance to abiotic stresses in Agriculture: Role of Genetic Engineering, Kluwer Academic Publishers, Netherlands, pp 201-222.

Short Communications

Short Communications are limited to a maximum of two figures and one table. They should present a complete study that is more limited in scope than is found in full-length papers. The items of manuscript preparation listed above apply to Short Communications with the following differences: (1) Abstracts are limited to 100 words; (2) instead of a separate Materials and Methods section, experimental procedures may be incorporated into Figure Legends and Table footnotes; (3) Results and Discussion should be combined into a single section.

Proofs and Reprints: Electronic proofs will be sent (e-mail attachment) to the corresponding author as a PDF file. Page proofs are considered to be the final version of the manuscript. With the exception of typographical or minor clerical errors, no changes will be made in the manuscript at the proof stage.

International Journal of Physical Sciences

Table of Contents: Volume 8 Number 41, 9 November, 2013

ARTICLES

Predicting geotechnical parameters of fine-grained dredged materials of the gulf of Izmit (NW Turkey) using the slump test method and index property correlations 1944
Kurtulus C., Bozkurt A. and Endes H.

Theoretical and experimental studies for wool wax recovery by flotation 1954
Mohsen A. Hashem and Mohammednoor N. Almaghrabi

Optimal lead-lag controller designing for reduction of load current total harmonic disturtion and hanmonic with voltage control using honey bee mating optimization (HBMO) 1966
Hamdi Abdi and Ramtin Rasoulinezhad

academicJournals

Vol. 8(41), pp. 1944-1953, 9 November, 2013
DOI: 10.5897/IJPS11.1153
ISSN 1992 - 1950 © 2013 Academic Journals
http://www.academicjournals.org/IJPS

International Journal of Physical Sciences

Review

Predicting geotechnical parameters of fine-grained dredged materials of the gulf of Izmit (NW Turkey) using the slump test method and index property correlations

Kurtulus C.[1]*, Bozkurt A.[2] and Endes H.[1]

[1]Department of Geophysics, Kocaeli University, Engineering Faculty, Izmit-Kocaeli, Turkey.
[2]ABM Engineering Co., Izmit-Kocaeli, Turkey.

Accepted 8 November, 2013

In this study, an attempt has been done to figure out the geotechnical properties of physically remolded dredged materials of the Gulf of Izmit located in NW Turkey, by using slump test method. For this aim, slum tests were conducted on dredged material specimens using open-ended polyvinyl chloride (PVC) cylinders of 10 cm diameter and height. Water content of the dredged material specimens was obtained in the laboratory using oven method. Bulk wet density, Atterberg limits and phase relations such as bulk unit weight, % solids by weight, void ratio, and engineering behavior properties such as Vane shear strength, and effective stress were determined. Later, the statistical correlations were conducted by regression analysis to obtain the relationships between water content and slump/cylinder height as well as other parameters such as wet bulk density, % solid by weight, void ratio, Vane shear strength and effective stress.

Key words: Vane shear strength, dredged materials, slump test.

INTRODUCTION

Description of dredged material properties is very necessary for any planned dredging operation, and the fundamental geotechnical parameters need to be determined or predicted. While near shore dredging operations, the dredging process generally involves too much material handling, manipulation, and remolding. The natural previously deposited material has been dredged, transported and re-deposited by the time. Therefore, its geotechnical properties are changed. The most fundamental parameters of the dredged materials are grain size distributions, water content, density, specific gravity and percent solid. Engineering properties include shear strength, permeability, viscosity, consolidation and critical erosion.

The laboratory tests of soil classification and description, grain size analysis and distribution, specific gravity of solid particles, water content, bulk density, shear strength, stress-strain and behavior characteristics provide basic information about the dredged material soil properties. Dredged materials lose their original geotechnical properties while they are being dredged, transported and redeposited. Intergranular bonding and physico-chemical condition affect the materials behavior (Mitchell, 1993; Lee, 2004). As the water content in the dredged material is increased during remoulding and the solid particles become more separated, the material behaves like slurry. If fine-grained particles (silt and clay) composed more than 35% of the total matrix solids, the slurry behaves as viscous material (Spigolon, 1993). High organic content, gas bubbles and fibrous materials affect the shear strength of dredged materials (Klein and Sarsby, 2000; Edil and Wang, 2000). DeMeyer and Mahlerbe (1987) determined the threshold (yield) shear stress σ most clayey slurries less than 10 Pa. Bouziani

*Corresponding author. E-mail: cengizk@kocaeli.edu.tr, Tel: +90-262-303 31 04. Fax: +90-262-303 31 02.

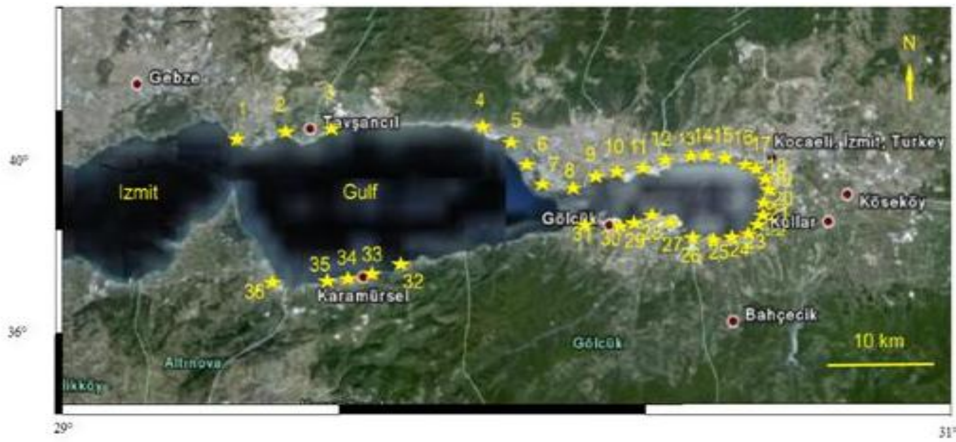

Figure 1. Study area. Stars indicate the dredged material collection points (Google earth).

and Benmounah (2013) conducted v-funnel and mini-slump tests with viscosity of Self-Compacting Mortars (SCM), measured at different rotational speeds and linear relationships were obtained between both v-funnel and mini-slump tests and viscosity. Peila et al. (2009) performed the slump cone test on conditioned material to check the mass behavior. Vinai et al. (2008) used a simple slump test to analyze the global characteristics of the conditioned soils.

The dredged materials are used to improve soil structure for agriculture purposes. Some dredged materials may be very good topsoil according to Francingues et al. (2000) and Nelson and Pullen 1990). They are also used for creating embankments (McLellan et al., 1990; Smith and Gailani, 2005), land improvement (Harrison and Luik, 1980; Perrier et al., 1980; Spaine et al., 1978), land creation (Coastal Zone Resources Division, 1978; capping (Palermo et al., 1998), replacement fill and share protection (Comoss et al., 2002).

The advantage of the slump test is that it allows rapid field estimation of a material's water content (with calculated void ratio, density, or other phase relationships) if a previously developed slump-water content curve is available for the given material. The slump test was originally developed for rapid estimation of mine tailing properties in Australia (University of Melbourne, 1996) by observing the height drop (slump) instead of the spread diameter. In this study, slump tests were conducted on 36 dredge material specimens collected along the coastal areas of the Gulf of Izmit (Gürbüz and Gürer, 2008). Index parameters, phase relationships and engineering behavior of the specimens were determined and some correlations were performed.

Study area

The study was performed at the coastal areas of the Gulf of Izmit, located NW Turkey (Figure 1).

Gulf sediment specimens

The dredged material specimens were collected using a small dredging operation from the study area for the purpose of characterizing their geotechnical properties. The grain size distribution graphic of the dredged material specimen collected from Station #1 is given in Figure 2 and the grain size distribution values of specimens collected from 36 stations are given in Table 1.

The slump test method

The slump test is an operation that consists of filling an upright open-ended cylinder with remolded dredged material, getting rid of the excess material at the top; slowly lifting the cylinder and measuring the variation in height (slump) as the material complete its outward flow. The slump test for concrete (ASTM 2000a) has been used for years to measure the consistency of freshly mixed concrete for quality control purposes. For this test a conical upright open ended cylinder is filled with wet concrete and tamped with a rod. After removing the excess material at the top, the cylinder is slowly lifted and the resulted variation in height (slump) of the concrete is measured. The open-ended cylinder size is 150 mm in height, with a 76 mm inside diameter.

Slump test application

Slump tests were conducted on 36 dredged material specimens using an open-ended polyvinyl chloride (PVC) cylinder of 10 cm height and diameter. *In situ* each dredge material specimen was placed into the slump cylinder, leveled off, and allow to flow outward as the cylinder was slowly lifted upward with minimum disturbance to the specimen. After the outward flow has visually stopped, the change in height (slump) as material

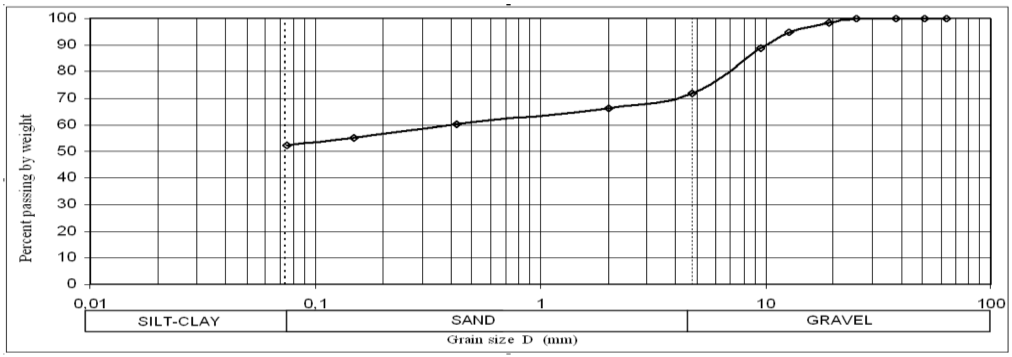

Figure 2. Grain size distribution of dredged specimen collected from Station #1.

Table 1. Grain size distribution of specimens collected from 36 stations.

Station No	Gravel	Sand	Silt+Clay
1	28.31	19.32	52.36
2	30.12	19.61	50.27
3	25.63	21.10	53.27
4	26.58	23.17	20.26
5	29.15	17.94	52.91
6	30.81	17.43	51.76
7	25.94	22.78	51.28
8	28.91	20.45	50.64
9	28.64	15.13	56.23
10	29.48	19.65	50.87
11	29.11	17.39	53.47
12	31.92	15.11	52.98
13	25.48	21.89	52.63
14	26.45	23.15	50.32
15	25.31	20.87	53.82
16	27.96	21.69	50.36
17	21.93	23.76	54.31
18	23.81	23.84	52.36
19	16.34	20.47	63.19
20	21.59	19.52	58.49
21	19.78	25.49	54.73
22	23.62	25.02	51.36
23	12.56	25.11	62.34
24	23.58	25.45	50.96
25	21.36	25.74	52.63
26	22.54	26.79	50.67
27	22.45	22.07	55.48
28	24.51	24.06	51.43
29	24.73	20.59	54.68
30	25.31	24.45	50.23
31	26.94	18.70	54.36
32	38.14	11.74	50.12
33	29.57	19.00	51.43
34	31.96	17.36	50.68
35	19.74	26.47	53.79
36	21.65	28.06	50.29

completes its outward flow is measured. The slump was divided by cylinder height to find normalized slump which is the best predictor (DOER, 2004), (Figure 3). The slump test was performed as quickly as possible to prevent thixotropic effects. The cylinder walls were pre-wetting to prevent material sticking to the walls while lifting the cylinder. The cylinder was removed in less than *7* s after leveling off the top.

Determination of water content *(Wn)* and bulk wet density *(γ)*

The water content is the ratio of the weight of water to weight of solids obtained by weighing a specimen in its natural wet state and then again upon drying at 105°C for 24 h. Bulk wet density was obtained using Equation 1.

$$Wn(\%) = 2.10^{11}\gamma^{-4.7128} \quad (1)$$

The relationship between *Wn (%)* and normalized slump (slump/cyl ht) is given in Figure 4. The water content and normalized slump data show scattering since the coarser-grained soils have less water content variability. The relationship between water content and bulk wet density is illustrated in Figure 5.

Determination of Atterberg limits

The Atterberg limits are a basic measure of a fine-grained soil consisting of the liquid limit (water content at which the soil passes from the liquid to plastic state), the plastic limit (water content at which the soil passes from the plastic to semi-solid state) and the shrinkage limit (water content at which the soil passes from the semi-solid to the solid state). Laboratory testing (ASTM, 2000b) is required to determine the Atterberg limits. A suitable prediction method using water content percent and normalized slump is given by the Equation 2 (DOER-D1, 2004).

$$LL = 52.74 + 0.526Wn - 59.97\ N \quad (2)$$

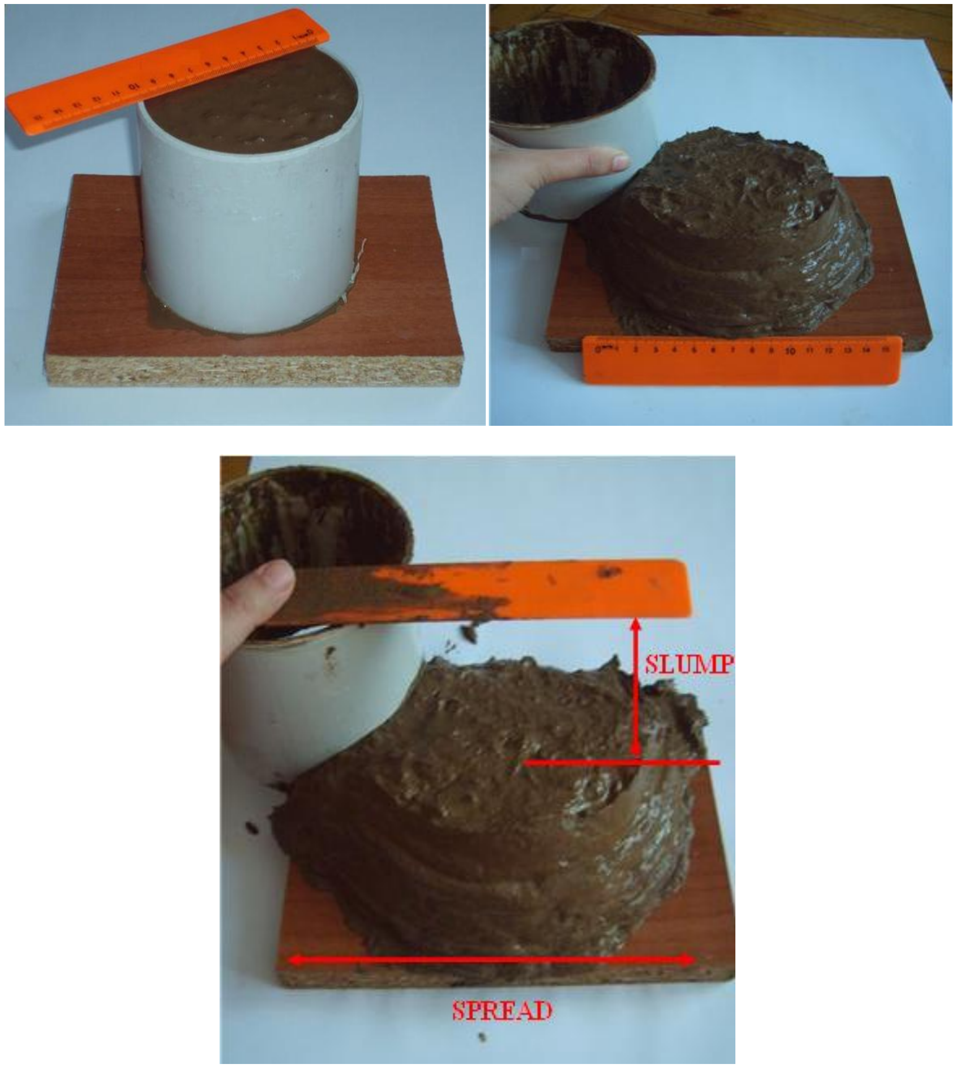

Figure 3. Sequences of slump test application.

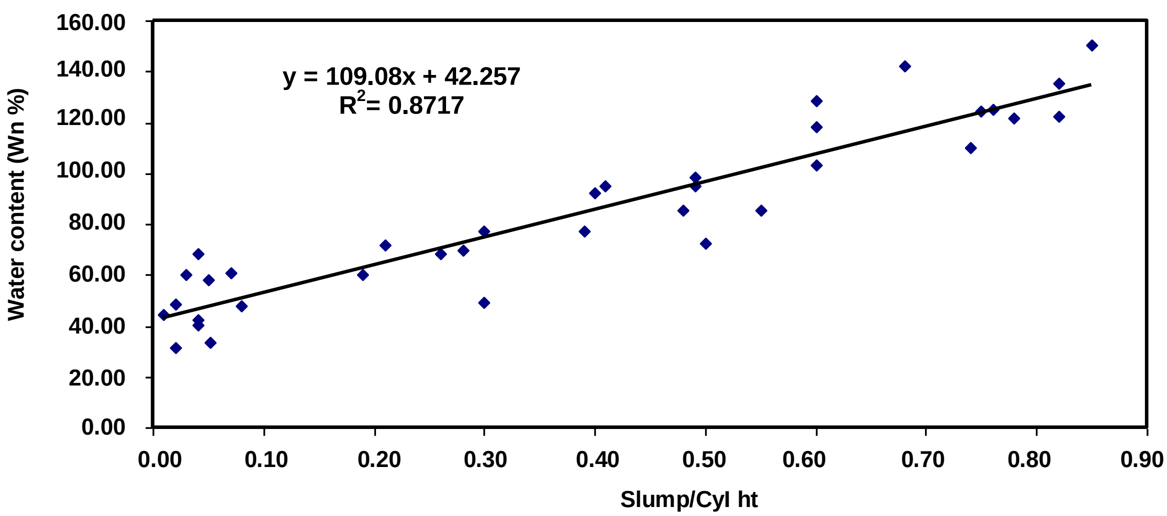

Figure 4. Relationship between water content and normalized slump.

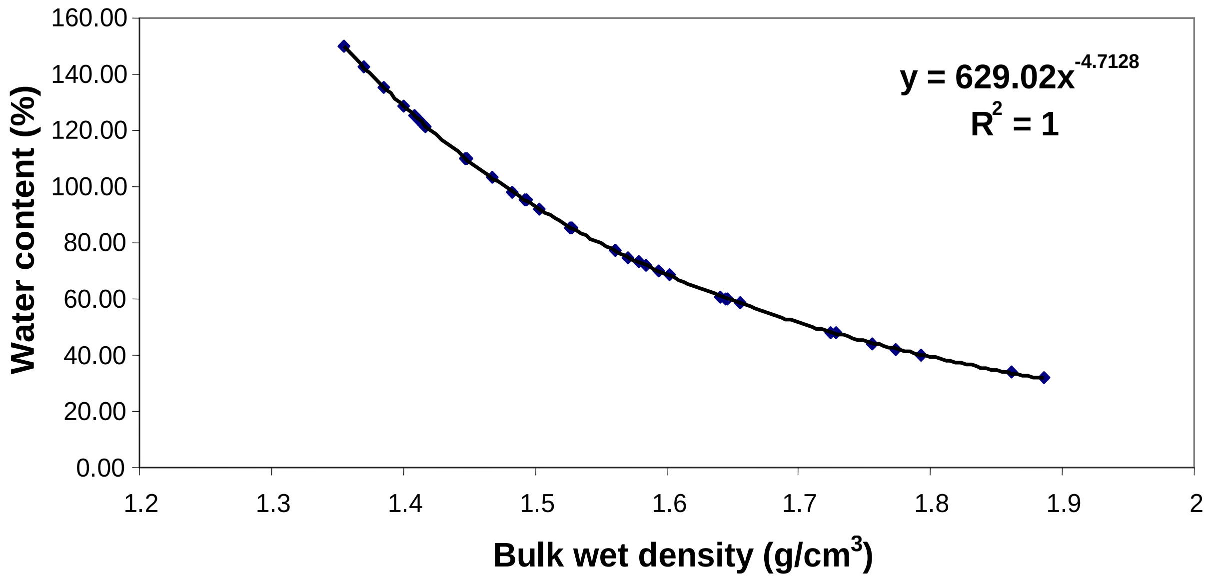

Figure 5. The relationship between water content and bulk wet density.

Where, LL: Liquid limit percent, W: Water content percent, N: Normalized slump = (slump / cylinder height). Liquidity index (LI) and Plastic limit percent (PL) are given by Equations 3 and 4.

$$LI = 1.601(Wn/LL) - 0.612 \quad (3)$$

$$PL = [(LI)(LL) - Wn]/[(LI) - 1] \quad (4)$$

Plasticity index (PI) is obtained from the difference of LL and PL Equation 5.

$$PI = LL - PL \quad (5)$$

The Atterberg limits of the dredged material specimens were figured out using Equations (2 to 5). The results are given in Table 2.

Determination of bulk unit weight (saturated wet bulk density), (γ)

The Equation (6) is used to determine the bulk unit weight of the dredged material when only the water content is known (DOER-D1, 2004).

$$\gamma = 233.21\omega^{-0.2051} \quad (6)$$

Where, γ: Bulk unit weight (N/m^3), *Wn*: Water content percent .

The result of bulk unit weight of dredged material specimens determined using Equation (6) is given in Table 2.

Determination of void ratio *(e)*

Void ratio *(e)* is defined as the ratio of the volume of voids to the volume of solids. If only water content is known, the void ratio can be easily determined conducting a single slump test and using Equation 7.

$$e = 0.028\,Wn - 0.055N - 0.065 \quad (7)$$

Where, *e*: Void ratio, *Wn*: Water content percent, *N:* slump / cylinder height.

The void ratio data of dredged material specimens determined using Equation (7) is given in Table 2.

Determination of percent solids

General equation for percent solids by weight is given by Equation (8) (DOER-D1, 2004).

$$\%\ solids\ by\ weight = 10000/(Wn + 100) \quad (8)$$

Where, *Wn*: Water content percent.

The percent solids by weight obtained using Equation (8) are given in Table 2. The relation between % solids by weight and water content is shown in Figure 6.

Determination of specific gravity

Specific gravity is the ratio of density of a substance compared to the density of fresh water at 4°C (39°F). Specific gravity compares the mass of a given volume of material to the mass of the same volume of water and

Table 2. Physical properties of dredged material specimens collected from the coastal areas of the Gulf of Izmit.

Specimen No.	Slump/Cyl ht	Solid weight (%)	Water content (%)	Wet bulk density (N/m³)	Liquid limit (%)	Liquidity index	Plastic limit (%)	Plasticity index
1	0.02	75.94744	31.67	1.885489	68.19902	0.131466	26.14076	42.05826
2	0.04	70.28395	42.28	1.773361	72.58048	0.320624	27.98004	44.60044
3	0.07	62.14268	60.92	1.641114	80.58602	0.598296	31.62955	48.95647
4	0.08	67.71398	47.68	1.728704	73.02208	0.433378	28.29723	44.72485
5	0.40	52.04267	92.15	1.503146	77.2229	1.298472	27.21109	50.01181
6	0.41	51.25051	95.12	1.493062	78.18542	1.335769	27.75018	50.43524
7	0.49	50.45154	98.21	1.482968	75.01316	1.484088	27.09455	47.91861
8	0.30	56.43978	77.18	1.560765	75.34568	1.027977	9.780324	65.56536
9	0.60	43.73305	128.66	1.400376	84.43316	1.827618	30.99445	53.43871
10	0.03	62.41808	60.21	1.645201	82.61136	0.554864	32.28662	50.32474
11	0.01	69.30487	44.29	1.75597	75.43684	0.327969	29.08951	46.34733
12	0.02	67.43998	48.28	1.724123	76.93588	0.392684	29.75138	47.1845
13	0.55	53.8648	85.65	1.526658	64.8084	1.503862	23.44472	41.36368
14	0.49	51.18755	95.36	1.492264	73.51406	1.464764	26.5097	47.00436
15	0.50	50.47701	72.48	1.483289	62.205	1.500322	50.95218	11.25282
16	0.60	47.62585	118.45	1.447803	74.60222	1.74801	15.98296	58.61926
17	0.04	57.72339	68.38	1.578215	88.86544	0.707492	18.83166	70.03378
18	0.05	63.15125	58.35	1.656192	80.4336	0.549434	31.42054	49.01306
19	0.04	71.33685	40.18	1.792635	71.47588	0.287998	27.52109	43.95479
20	0.052	74.8111	33.67	1.861147	67.33198	0.188595	25.84592	41.48606
21	0.60	49.20049	103.25	1.467304	71.0675	1.714003	25.99419	45.07331
22	0.68	41.26093	142.36	1.37063	85.04266	2.068047	31.37712	53.66554
23	0.82	42.50436	135.27	1.385568	74.71662	2.286515	27.64887	47.06775
24	0.85	39.96483	150.22	1.355089	80.78122	2.365205	29.91794	50.86328
25	0.26	62.0232	68.35	1.639348	76.6981	0.814741	31.63624	45.06186
26	0.21	59.98081	48.22	1.609749	89.4126	0.677214	35.46784	53.94476
27	0.30	55.16328	82.33	1.543717	57.8769	15.58019	23.31408	34.56282
28	0.39	54.77951	77.12	1.538647	69.91682	1.153943	23.12561	46.79121
29	0.28	60.09254	56.32	1.61134	72.7684	0.928092	34.26943	38.49897
30	0.19	62.3558	48.33	1.644275	72.9057	0.705592	29.06953	43.83617
31	0.82	44.98021	122.32	1.415473	67.90492	2.271949	25.12405	42.78087
32	0.74	46.41233	110.29	1.432914	66.37474	2.048263	24.48139	41.89335
33	0.75	45.41739	124.12	1.420784	73.04962	2.10829	26.96926	46.08036
34	0.78	45.14061	121.53	1.41742	69.88818	2.172012	25.82564	44.06254
35	0.76	44.38132	125.32	1.408214	73.08112	2.133406	26.99093	46.09019
36	0.48	53.95489	85.34	1.527833	68.84324	1.372644	24.57378	44.26946

Specimen No	Void radio	Specific gravity	Water content / Liquid limit	Vane shear (kPa)	Effective stress (kPa)	Undrained Shear strength (Cu) kN/m2	Compression index Cc	Permeability m/sec
1	0.82066	2.591285	0.464376	0.332503	230.2969	92.86217	0.523791	0.003877
2	1.11664	2.64106	0.582526	0.251262	79.27978	38.90342	0.563224	0.012674
3	1.63691	2.686983	0.755962	0.166543	23.26455	10.84738	0.635274	0.053101
4	1.26564	2.654446	0.652953	0.212619	46.34254	23.16091	0.567199	0.020351
5	2.4932	2.705589	1.193299	0.059043	2.716764	0.433202	0.605006	0.247325
6	2.57581	2.707958	1.216595	0.05587	2.48056	0.364911	0.613669	0.277925
7	2.65793	2.706374	1.309237	0.044851	1.756347	0.184464	0.585118	0.310768
8	2.07954	2.694403	1.024345	0.088135	5.571432	1.503198	0.588111	0.131322
9	3.50448	2.72383	1.523809	0.026966	0.860068	0.037992	0.669898	0.828806
10	1.61923	2.689304	0.728834	0.177608	27.62866	13.24592	0.653502	0.051026
11	1.17457	2.651998	0.587114	0.248544	76.4072	37.61104	0.588932	0.015356
12	1.28574	2.66309	0.627536	0.225828	55.86003	27.92821	0.602423	0.0216
13	2.30295	2.688792	1.321588	0.043557	1.680454	0.168427	0.493276	0.18565
14	2.57813	2.703576	1.297167	0.046154	1.834566	0.20161	0.571627	0.27865
15	2.0075	2.676667	1.577204	0.063114	2.587881	0.395421	0.469845	0.11052

Table 2. Contd.

16	2.98116	2.710885	1.474085	0.023172	1.005341	0.054792	0.58142	0.473262
17	1.98352	2.708247	0.824167	0.16129	15.49562	6.564475	0.709789	0.109923
18	1.56605	2.68389	0.725443	0.179042	28.24155	13.58087	0.633902	0.045089
19	1.05784	2.632753	0.562148	0.263701	93.73778	45.20208	0.553283	0.010314
20	0.8749	2.598456	0.50006	0.305527	162.5673	71.40371	0.515988	0.004971
21	2.793	2.705085	1.452844	0.031907	1.076385	0.064069	0.549608	0.370797
22	3.88203	2.726911	1.673983	0.018887	0.552708	0.012573	0.675384	1.187243
23	3.67746	2.718607	1.810441	0.013666	0.382288	0.004603	0.58245	0.981706
24	4.09441	2.725609	1.859591	0.012163	0.337026	0.003205	0.637031	1.430452
25	1.8378	2.688808	0.891156	0.120866	10.72872	4.008339	0.600283	0.081043
26	1.93835	2.692153	0.805256	0.148171	17.28368	7.545382	0.714713	0.098779
27	4.1185	2.745667	0.850426	0.133122	0.070703	1.46E-05	0.430892	2.391568
28	2.07291	2.687902	1.103025	0.073135	3.933439	0.842157	0.539251	0.127336
29	1.8796	2.685143	0.961956	0.102187	7.487823	2.379808	0.564916	0.086991
30	1.60455	2.67425	0.822981	0.142073	15.60096	6.622081	0.566151	0.049257
31	3.31486	2.70999	1.801342	0.013964	0.391457	0.004922	0.521144	0.680927
32	2.98242	2.704162	1.661626	0.019449	0.572314	0.01377	0.507373	0.468257
33	3.36911	2.714397	1.699119	0.017794	0.515283	0.010448	0.567447	0.721164
34	3.29494	2.711215	1.738921	0.016192	0.462103	0.007794	0.538994	0.666602
35	3.40216	2.714778	1.714807	0.017145	0.493479	0.009308	0.56773	0.746438
36	2.29812	2.692899	1.239628	0.0529	2.271074	0.307983	0.529589	0.184358

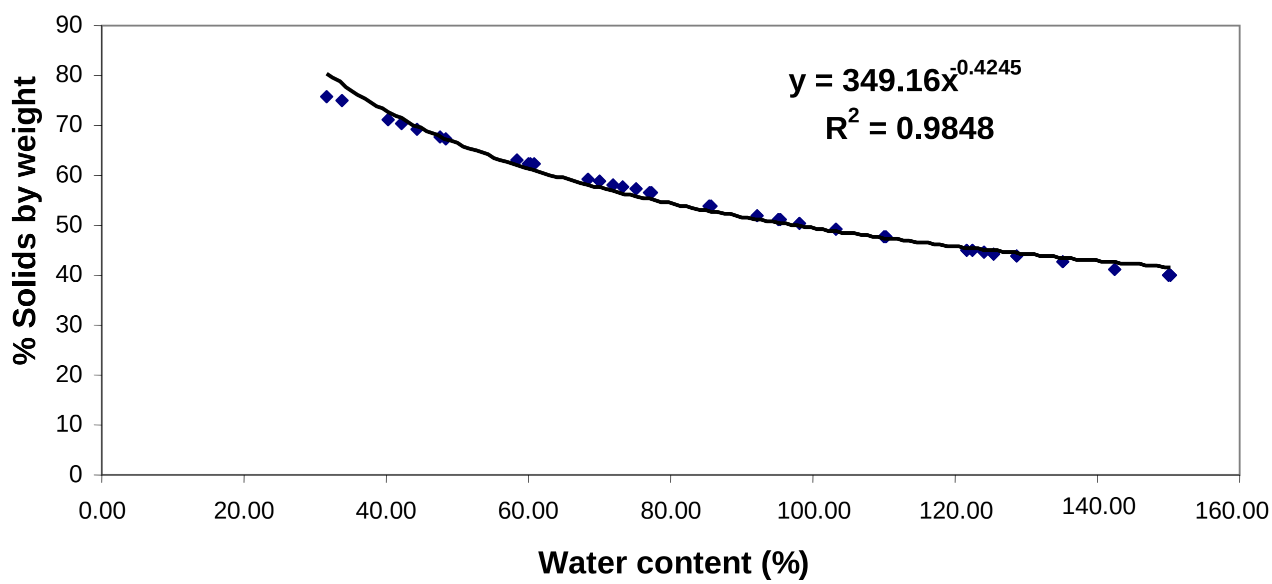

Figure 6. Relationship between % solids by weight and water content.

helps determine types of the minerals. Specific gravity is calculated from Equation 9.

$$Gs = 2.8 - 5.5\ N/W - 6.5/W \quad (9)$$

Where, *Gs*: Specific gravity of solids, *W*: Water content percent, *N*: Normalized slump=slump/cylinder height.
The specific gravity values are given in Figure 2.

Determination of undrained shear strength (c_u)

If only the water content and liquid limit of the dredged material are known, the undrained shear strength is obtained using the approximate Equation 10, (DOER-D1, 2004).

$$LI = \log(170/c_u)/2 \quad (10)$$

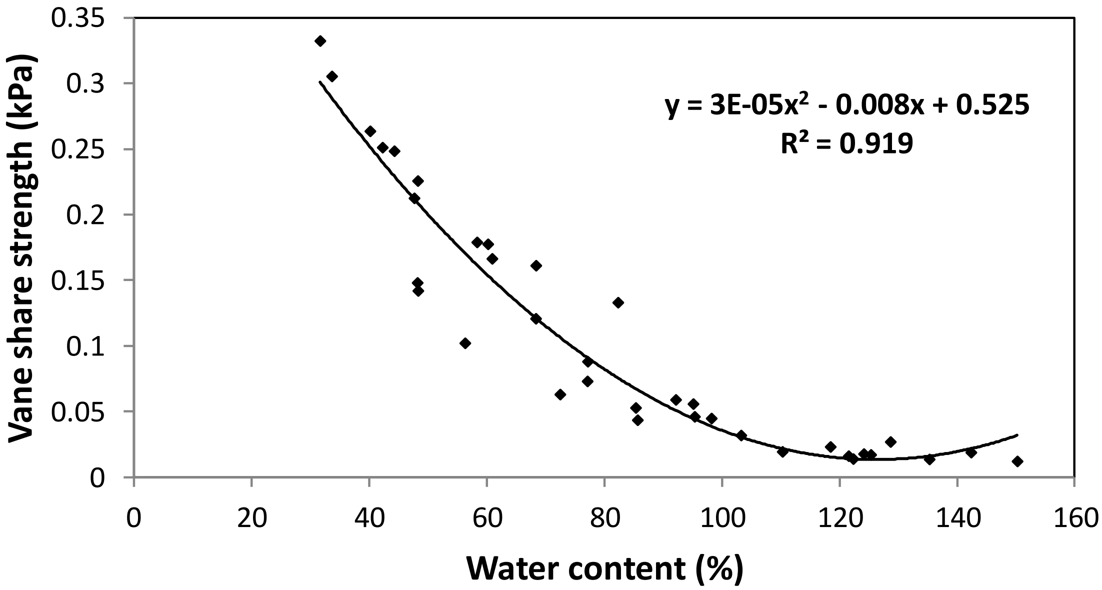

Figure 7. Relation between Vane shear strength and water content (%) / LL.

$$C_u = 170e^{-4.6LI} \quad (11)$$

Where *LI*: Liquidity bindex, c_u: Undrained shear strength

$$e = 2.178$$

The soil compression index Cc is given by Equation 12 (Terzaghi and Pack, 1967).

$$Cc = 0.009(LL - 10) \quad (12)$$

Where *Cc*= Compression index, *LL*= Liquid limit percent.

Determination of Vane shear strength

The Vane test is one of the most widely used techniques to estimate the undrained strength of soft clays. It provides an indication of *in-situ* undrained shear strength of fine - grained clays and silts or other fine geomaterials such as mine tailings, organic muck, and substances where undrained strength determination is required. It is a cheaper and quicker method. Vane shear strength is given by Equation 13.

$$Vane\ shear\ strength = 183e^{-2.3714\,(Wn/LL)} \quad (13)$$

Where, *e:* 2.718, Wn/LL: Water content percent / Liquid limit percent.

The Vane shear strength values determined are given in Table 2, and the relation between Vane shear strength and water content (%) / *LL* is demonstrated in Figure 7.

As depicted in Figure 7, the correlation between Vane shear strength and water content (%) / *LL* is very good.

Determination of effective stress (σ')

The effective stress is a combination of both the externally applied stresses and the internal pressure of fluid phase(s) and enables the conversion of a multiphase porous medium into mechanically equivalent single-phase continuum. Soil settlement models are developed base on effective stress concept where settlement is always associated with effective stress increase (Terzaghi, 1943; Janbu et al., 1956; Schertmann et al., 1978). If only the water content percent and liquid limit are known, then the effective stress is calculated by Equation 14 (DOER-D1, 2004).

$$\sigma' = 129.77(Wn/LL)^{-4.7044} \quad (14)$$

Where, σ': Effective stress (kPa), *Wn /LL*: Water content percent / liquid limit percent.
The calculated effective stress values are given in Table 2, and the relation between effective stress and water content / liquid limit is shown in Figure 8.

Determination of permeability *(k)*

Permeability is determined by Equation 15.

$$k = 0.0174\,[e - 0.027\,(PL - 0.242PI)\,/\,PI]^{4.29} / (1 + e) \quad (15)$$

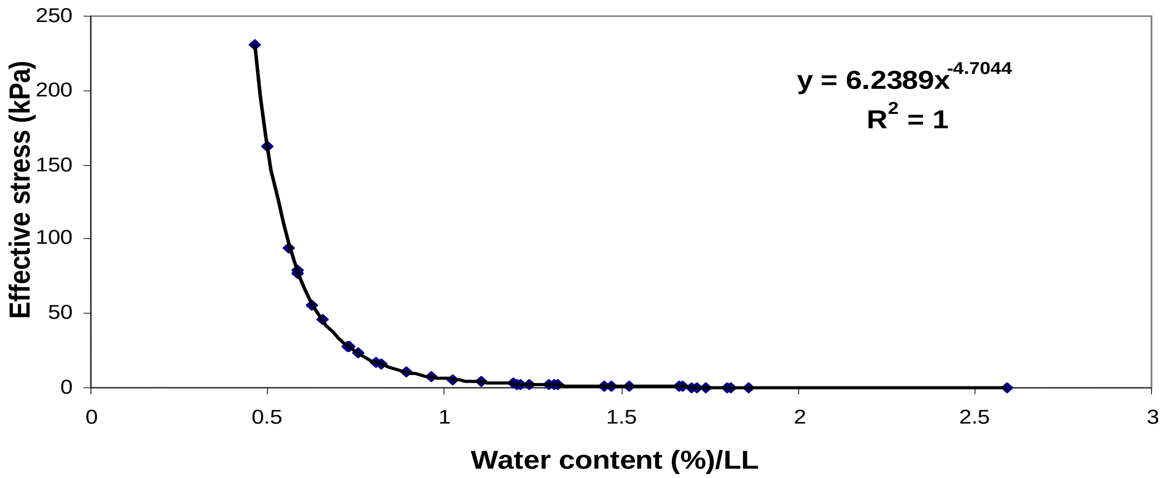

Figure 8. Relation between effective stress and water content / liquid limit.

Where, *k*: permeability, *e*: Void ratio, *PL*: Plastic limit percent, *PI*: Plasticity index.

DISCUSSION

The physical and engineering properties of the dredged materials collected at the coastal areas of the Gulf of Izmit were predicted using correlation equations given by ERDC TN-DOER (2004) in order to figure out their usability in engineering planning and construction aspect. These properties mostly depend upon the site geology. The dredged materials consist of mostly clay and silt which have plasticity index values change in a large range indicating medium to very high plasticity. They have relatively high water content and void ratio but very low shear strength indicating that they are very soft in consistency. These results show similarities with the results obtained by ERDC TN-DOER (2004) and Klein and Sarsby (2000). The water content and bulk wet density obtained by ERDC TN-DOER (2004) are higher than our values. This study is the first study on the marine dredged materials at the coastal areas of the Gulf of Izmit. The results obtained in this study can be utilized by the researchers and the people who are interested in dredged materials.

CONCLUSIONS

In order to determine the physical and geotechnical properties of dredged materials of the Gulf of Izmit, a combination of slump tests were conducted *in-situ* and water content of the dredged material specimens were obtained in the laboratory using the oven method. The other properties such as bulk wet density, Atterberg limits, bulk unit weight, void ratio, percent solids, shear strength and effective stress were calculated using the formulae given by Doer Technical Note (ERDC TN-DOER-D1, 2004).

Sieve analysis indicated that the dredged material had 12.56 to 30.12% gravel, 11.74 to 28.06% sand and 20.26 to 63.19% clay and silt. Atterberg limit tests demonstrated that the dredged material had liquid limit ranging from 57.86 to 89.41, plastic limit varying from 9.78 to 50.95 and plasticity index ranging from 11.25 to 70.03. The specific gravity of the dredge material varied from 2.59 to 2.72. The natural water content ranged from 31.67 to 150.22% with the void ratio changed from 0.82 to 4.11. The Vane shear strength varied from 0.013 to 0.33 kg/cm^2. The effective stress ranged from 0.07 to 230.29 kg/cm^2. The dredged material was very soft in consistency and exhibit very low shear strength.

Good correlations were determined ($R^2 = 0.87$) between water content and normalized slump, % solids by weight and water content ($R^2 = 0.98$) and Vane shear strength and water content/liquid limit ($R^2 = 0.872$). Very good correlations were obtained between water content and bulk density and effective stress and water content/liquid limit ($R^2 = 1$). Water content increases with increasing slum/Cyht, and exponentially decreases with increasing bulk wet density. % solids by weight and Vane shear strength decrease exponentially with increasing water content. Similarly the effective stress also decreases exponentially with increasing water content/LL. The geotechnical parameters using the correlation equations are for the preliminary investigations and do not substitute for standardized laboratory testing requirements.

REFERENCES

ASTM (2000a, b). The standard American Society for Testing and Materials.

Bouziani T, Benmounah A (2013). Correlation Between V-funnel and Mini-slump Test Results with Viscosity, KSCE J. Civil Eng. DOI 10.1007/s12205-013-1569-1, 17(1):173-178.

Coastal Zone Resources Division (1978). Handbook for Terrestrial Wildlife Habitat Development on Dredged Material, Technical Report D-78-37, U.S. Army Engineer Waterways Experiment Station, Vicksburg, MS.

Comoss EJ, Kelly DA, Leslie HZ (2002). Innovative Erosion Control Involving the Beneficial Use of Dredged Material, Indigenous Vegetation and Landscaping Along the Lake Erie Shoreline, Ecological Engineering. 19:203-210.

DeMeyer CP, Mahlerbe B (1987). Optimization of maintenance dredging operations in maritime and estuarine areas, Terra et Aqua, International Journal on Public Works, Ports, and Waterways Developments, Int. Assoc. Dredging Companies. 35:25-39.

Doer Technical note collection, (ERDC TN-DOER-D1: 2004, August).

Edil TB, Wang X (2000). Shear strength and Ko of peats and organic soils, Geotechnics of high water content materials, ASTM STP 1374, T.B. Edil and P.J. Fox, eds., American Society for Testing and Materials, West Conshohocken, PA. 209-225.

Francingues NR, McLellan TN, Hopman RJ, Vann RG, Woodward TD (2000). Innovations in dredging technology: equipment, operations and management, DOER Technical Notes Collection (ERDC TN-DOER-T1), U.S. Army Research and Development Center.

Gürbüz A, Gürer ÖF (2008). Tectonic Geomorphology of the North Anatolian Fault Zone in the Lake Sapanca Basin (Eastern Marmara Region, Turkey). Geosci. J. 12 (3): 215-225.

Harrison W, Luik A (1980). Suitability of Dredged Material for Reclamation of Surface-mined Land, Ottawa, Illinois, Demonstration Project, Technical Report EL-80-7, U.S. Army Engineer Waterways Experiment Station, Vicksburg, MS.

Janbu N, Bjerrum L, Kjaernsli B (1956) "Veiledring ved losning av fundermenteringsoppgaver." Norwegian Geotechnical Institute Publication. (16), Oslo.

Klein A, Sarsby RW (2000). Problems in defining the geotechnical behavior of wastewater sludges, Geotechnics of high water content materials, ASTM STP 1374, T.B. Edil and P.J. Fox, eds., American Society for Testing and Materials, West Conshohocken, PA, 74-87.

Lee LT (2004). Predicting geotechnical parameters for dredged materials using the slump test method and index property correlation, DOER Technical Notes Collection (ERDC TN-DOER-D-X), U.S. Army Engineer Research and Development Center, Vicksburg, Mississippi.

Mclellan TN, Kraus NC, Burke CE (1990). Interim Design for Nearshore Berm Construction, Dredging Research Technical Notes, U. S. (DRP-5-02) Army Engineer Waterways Experiment Station, Vicksburg, MS.

Mitchell JK (1993). Fundamentals of soil behavior, 2nd ed., John Wiley & Sons, Inc., New York.

Nelson DA, Pullen EJ (1990). Environmental Considerations in Using Beach Nourishment for Dredged Material Placement, 113-128. In: R. L. Lazor and R. Medina (eds.) Beneficial Uses of Dredged Material. Technical Report D-90-3, U.S. Army Engineer Research Waterways Experiment Station, Vicksburg, MS.

Palermo MR, Clausner JE, Rollings MP, Williams GL, Myers TE, Fredette TJ, Randall RE (1998). Guidance for Subaqueous Dredged Material Capping, DOER Technical Report (DOER-1), U.S. Army Engineer Research and Development.

Peila D, Oggeri C, Borio L (2009). Using the Slump Test to Assess the Behavior of Conditioned Soil for EPB Tunneling, Environmental and Engineering Science, doi: 10.2113/gseegeosci.15.3.167 15(3):167-174.

Perrier E, Liopis J, Spaine P (1980). Area Strip Mine Reclamation Using Dredged Material A Field Demonstration, Technical Report EL-80-4, U.S. Army Engineer Waterways Experiment Station, Vicksburg, MS.

Schmertmann JH, Hartman JP, Brown PR (1978). "Improved strain influence factor diagrams." Proceedings, American Society of Civil Engineers, 104(GT8): 1131 – 1135.

Smith ER, Gailani JZ (2005). Nearshore Placed Mound Physical Model Experiment, DOER Technical Notes Collection (ERDC TN-DOER-D3), U.S. Army Engineer Research and Development Center, Vicksburg, MS.

Spaine PA, Liopis JL, Perrier ER (1978). Guidance for Land Improvement Using Dredged Material Synthesis Report, Technical Report DS-78-21, U.S. Army Engineer Research Waterways Experiment Station, Vicksburg, MS.

Spigolon SJ (1993). Geotechnical factors in the dredgeability of sediments, Reports 1 and 2, Contract Report DRP-93-3, U.S. Army Waterways Experiment Station, Vicksburg, MS.

Terzaghi K (1943) Theoretical soil mechanics. New York, Wiley Publications

Terzaghi K, Peck RB (1967). Soil Mechanics in Engineering Practice. A Wiley International Edition, P. 729.

Vinai R, Oggeri C, Peila D (2008). Soil conditioning of sand for EPB applications: A laboratory research. Tunnelling and Underground Space Technol. 23(3):308-317.

academicJournals

Vol. 8(41), pp. 1954-1965, 9 November, 2013
DOI: 10.5897/IJPS2013.3809
ISSN 1992 - 1950 © 2013 Academic Journals
http://www.academicjournals.org/IJPS

International Journal of Physical Sciences

Full Length Research Paper

Theoretical and experimental studies for wool wax recovery by flotation

Mohsen A. Hashem[1]* and Mohammednoor N. Almaghrabi[2]

[1]College of Engineering, Jazan University, P. O. Box 114 Jazan, Kingdom of Saudi Arabia.
[2]Mining Engineering Department, Faculty of Engineering, KING ABDULAZIZ UNIVERSITY, P.O. Box 80204 Jeddah, 21589 Kingdom of Saudi Arabia.

Accepted 5 November, 2013

Theoretical and experimental studies have been performed to analyze the flotation processes for recovery of wool wax from an industrial effluent by air flotation. Batch flotation process was carried out at different experimental conditions and different air flow rates. The results obtained show that wool wax can be successfully recovered from the tested effluent using batch air flotation. The percentage of wax recovery increased with increasing the flotation time, that 90% wax recovery was achieved within 10 min. These high recoveries reduce extraction costs. Wax recovery was found to decrease with increasing the initial concentration of wax/water emulsion. The highest percentage recovery of wax was obtained at a column working height approximately eight times the diameter of the flotation column at an emulsion of pH value of 9.0, inlet flow rate 1560 ml/min at a wool-soaping concentration 0.5 g/L. An appropriate kinetic model was identified to represent the behavior of wool wax recovery from an industrial effluent by air flotation.

Key words: Wool wax, recovery, air flotation, industrial effluents.

INTRODUCTION

During recent years there is an increasing public awareness concern regarding environmental pollution. Pollution is the contamination of environment as a result of human activities. The term pollution refers preliminary to the fouling of air, water and land by wastes. One of the major sources which can affect the quality of seas, rivers and underground water is oil and greases. Low concentration of oil or grease in seas and rivers impart an unpleasant taste to fish. Heavy surface grease films interfere with the process of natural aeration and photosynthesis. Free wax or oil and emulsions in water sources may coat their surface and destroy algae and other planktons thereby removing a source of fish food (Bateup et al., 1996; Christoe, 1986).

Millions head of sheep, the total sacrifice and sacrifice for the pilgrimage season every year in Kingdom of Saudi Arabia. A recovery process for removal of valuable wool wax as a product having the specification of lanolin from wool grease was found in the liquor from the scouring of raw wool. The process, apart from removing wool grease/wool wax from wool scouring effluent (Christoe et al., 1976; Kolattukudy, 1976; Moldovan et al., 2002), avoids the production of pollutants. And in the case of the treatment of wet sludge containing wool grease produces a virtually grease- free solid product suitable for disposal as an environmentally safe soil.

The cost of treatment of wax water emulsion by known processes such as those processes which rely on acid or

*Corresponding author. E-mail: drmohsen2@hotmail.com

base treatment or solvent extraction is quite high and in general have not proved economically attractive (Dominguez et al., 2003). However, the discarding of valuable and useable materials often found in the emulsion is unfortunate waste and in most cases the disposal of the emulsion to sewage systems and rivers is environmentally unacceptable without treatment of some sort (Anna et al., 2012). It may be practically useful to make some research efforts towards improvement of the performance in wax removal by simple operations and economic procedures (Max and Klaus, 1980).

Flotation processes have been proved (Rubio et al., 2002; Bradeley, 1985) suitable to remove both suspended solids and waxes at a time from a great variety of liquid water such as the effluents of pulp industry, the textile and dying industry, the food industry, the tannery process, the petrochemical industries (Tsubouchi et al., 1985), waste water, oil production, and refining electroplating and battery industries as well as, municipal waste water (Rippon, 1992). Flotation process is applicable to a wide range of oil water emulsions, which were found difficult to be processed by the known methods. Representative of these emulsion are the wool grease in water emulsions resulting from wool scouring processes. Flotation constitutes, thus an alternative process, which cover the advantages of concentration and separation method in one operation (Genon et al., 1984; Mercz and Cord-Ruwisch, 1997; Eychene et al., 2001).

Flotation processes are classified with respect to the method by which the air bubbles are generated as dissolved air flotation, induced air flotation, and electro flotation (Van Ham et al., 1983; Nicholas and Byeseda, 1980; Rajinder and Masliyan, 1983). The aim of the present work is to recover wool wax from industrial wool scouring effluents by air flotation using a batch flotation process, which is carried out at different conditions as preliminary steps for further continuous operation works. To suggest appropriate kinetic model to represent the behavior of wool wax recovery from an industrial effluent by air flotation.

EXPERIMENTAL

In order to obtain oil/water (W_x/W_a) emulsion, wool is first cleaned and then scoured (Gibson et al., 1981; McCracken and Chaikin, 1978). The obtained emulsion is treated by a flotation process at different conditions, of initial concentration, airflow rate, and the amount of soap used during the scouring process. Besides, both batch and continuous flotation are done at different feeding points. Within the scope of the present investigation discussion will emphasis on the batch flotation process only.

Materials

a) Wool: Raw wool, a protein (keratin), contains glandular secretions (suint and wool grease) and feces from the sheep, plus dirt, straw, and vegetable matter. Residues of treatments applied for disease control or for identification of the animal may also be present. Being amphoteric, wool is damaged by caustic or acid solutions, so special care is taken in processing.

b) Synthetic detergent: It reduces surface tension, increases the wetting capacity of the solution, converts the impurities of the fiber into emulsion and stabilizes the colloidal system formed (Athukorala and Mazza, 2011). In this work Nestabone, a local dispersing agent was used.

c) Soda soap and diethanolamine soaps: are used as foaming agent to create froth while diethanolamine is a soaping agent added for wax emulsification.

d) Soda ash,Na_2CO_3 (1%): Partially softens the water by interacting with calcium salts, creating an active reaction of the media which is most favorable for the formation of stable emulsion, and increase fiber swelling thus assisting the release of impurities from the fiber.

e) Caustic soda and nitric acid (Analar 99%), are used to adjust pH value

Emulsion stability test

Five W_x/W_a stocks solutions were prepared using 0.5 g of wool wax per liter of water. For all samples, mixing was continued for 60 min at a rate of 800 rpm, concentrations of emulsifier used were 200, 300, 400, 500 and 600 ppm. The samples were left to stand for 24 h each in a separate bottle, samples were taken from the surface and the bottom of each bottle and the turbidity was measured for each sample. The optimum amount of emulsifier required to attain 24 h stability was found to be 500 ppm.

Emulsion preparation

Ten wax/water emulsion concentrations were prepared by the following procedure (0.5 g of wool wax are added to 0.5 g of emulsifier in one liter of water and the resultant mixture is stirred for one hour at 800 rpm, a 500 ppm wax/water emulsion is obtained). A stock solution (250 ml) is diluted to one liter to obtain 125 ppm of oil in wax water emulsion. The turbidity is measured and recorded and the steps are repeated to prepare and measure 10 different concentrations of wax/water emulsion.

WAX WATER EMULSION PREPARATION

The procedure includes three main processes cleaning, scouring of wool and the flotation process. In the cleaning process 10 g of grey wool are boiled with 1 g synthetic detergent in 200 ml tap water for 7 min and then wool is removed from liquor. To that boiled wool sample 0.5 g soda soap powder are added in addition to 3 ml diethanolamine, 1 g synthetic detergent, 1 ml Na_2CO_3 solution (1%), and 200 ml tap water and the mixture is boiled for one hour. The resultant wool is washed, squeezed and the resultant squeezing off solution is added to the original mixture. The resulting emulsion is treated by the flotation process (Poole et al., 1999, Poole, 2004; Poole and Cord-Ruwish, 2004).

Flotation column and procedure

A column, 1 m height, 0.05 m diameter (Figure 1) with an opening for air inlet in the bottom was used, fitted with a sparger of 1 mm diameter for distributing of air into small bubbles. Along the column height there is a sampling opening and near the top of the column there is an outlet the foam. Accessory elements for the column are; pH meter, compressor, air flow meter and a pump. Results were

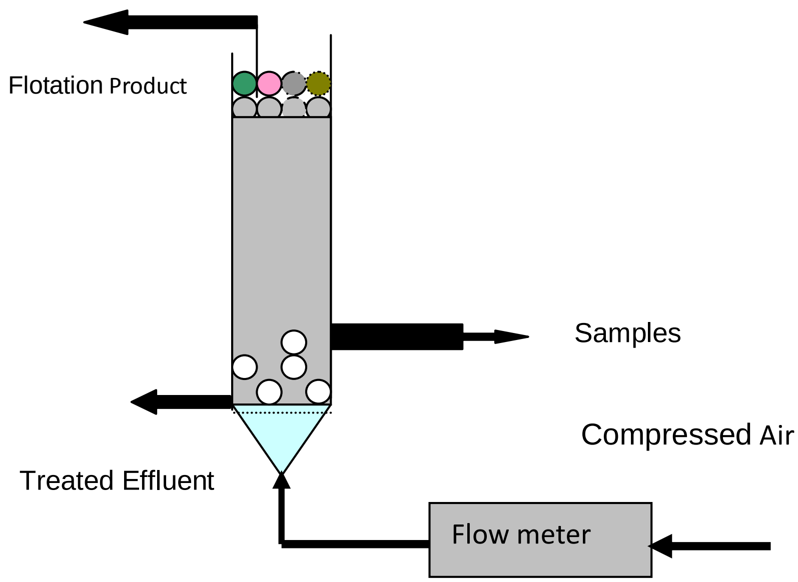

Figure 1. Sketch of flotation column.

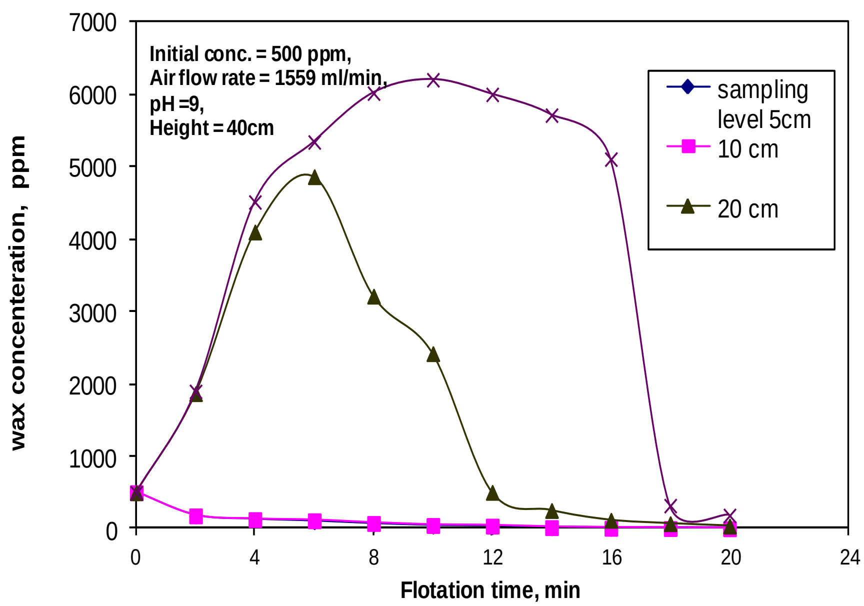

Figure 2. Effect of sampling level on wax concentration.

judged by a turbidity meter, measuring eFTU for comparison. The flotation column is washed thoroughly and is connected with all accessories required to begin an experiment. Turbidity and pH of the emulsion are measured before the flotation process. Different flotation experiments were carried out at different operating conditions such as initial concentrations of the W_x/W_a emulsion, working heights, inlet airflow rate, and different pH values. In all the experimental runs, samples are taken at 2 min intervals from different sampling points to measure the wax concentration.

RESULTS AND DISCUSSION

Effect of sampling point location

The effect of sampling point positions is clearly shown in Figure 2, which shows the relation between the wax concentration and time at different sampling points. It is clear that lowest wax concentration is obtained at the

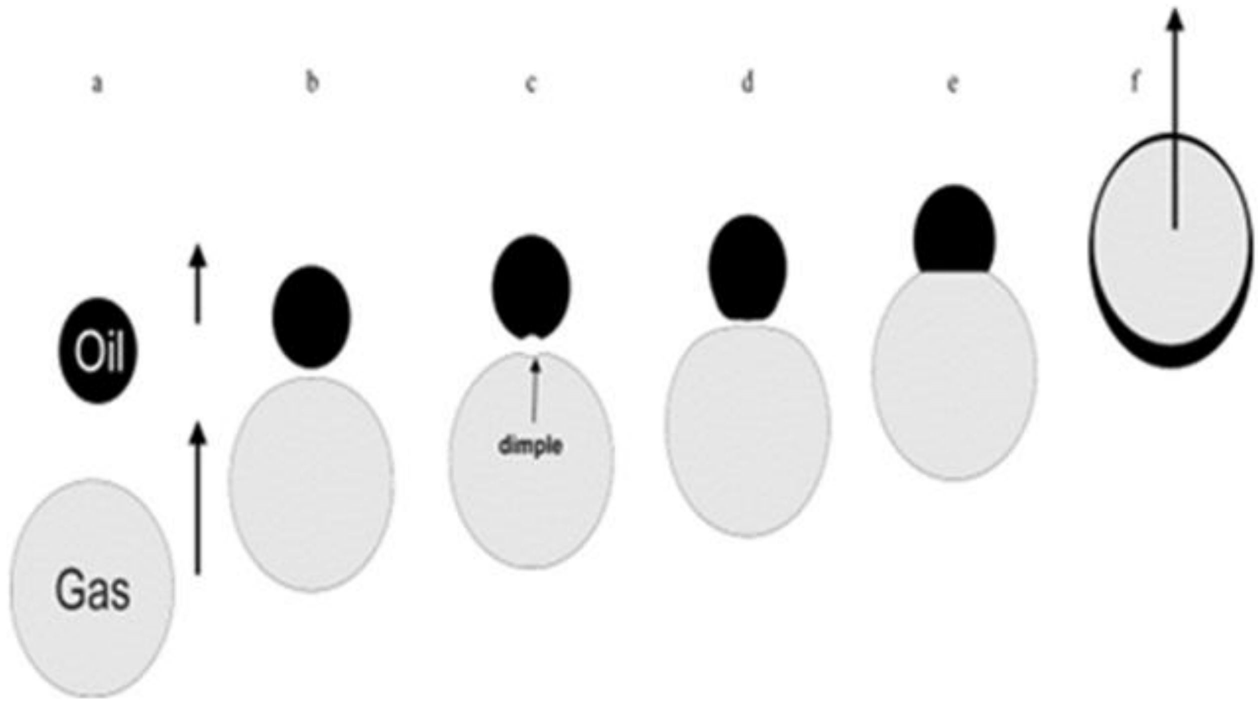

Figure 3. The attachment process. (a) Bubble and drop approach, (b) water film thinning, (c) thin film dimples due to interfacial tension gradients, (d) the dimples disappears as the film drains, (e) at a critical thickness film ruptures and if spreading conditions are present, the oil spread around the gas, (f) the conglomerate then continues to rise. If this processes have not occurred within the timeframe of approach, the bubble and drop do not attach but move away from each other.

lower sampling point and this is explained that gas flotation process may be an accelerated gravitational separation technique in which fine gas bubbles are injected into a water phase containing immiscible liquid droplets (wax) so that the gas bubbles (Figure 3) attach themselves to the wax droplets (Stewart, 1988a). The wax appears lighter because the density difference between the wax-air agglomerates and water is increased, consequently, the wax rises faster enabling a more rapid and effective separation from the aqueous phase. Air bubbles enter the flotation column near the lower sampling point where the bubbles are fresh and did not yet carry any wax so their ability to carry wax droplets is the highest along all the flotation column and so the wax concentration in the bottom of the column is the lowest one.

On the other hand at a height of 20 cm of the column top the wax concentration is increased with time until 6 min then with further increase in time the wax concentration is decreased. This is attributed to that after nearly 6 min all the wax droplets present in the column in the height below 20 cm are carried by air bubbles from the bottom of the column to the top. So the concentration of wax in the top is increased and with further increase in time there is no more wax droplets to be carried by the bubbles from the bottom. The air bubbles start to carry the oil droplets from height above 20 cm to the top of the column. Thus the wax concentration starts to reduce. The same holds with respect to the sampling point at height 40 cm at the start of the flotation process the air bubbles carried the oil droplets from the bottom of the column to the top of it till nearly most of the wax present in the bottom of the column is removed. The air bubbles start to carry the wax droplets from the top itself and so the wax concentration at the top of the column is increased at the start of the flotation process till time 16 min then with increasing the time the wax concentration is decreased.

Effect of different amount of soap

Figure 4 shows the effect of the different amount of soap used in the scouring process on the percent of wax removal during the flotation process. It is clear that as increasing the amount of soap the percent removal of the wax from the wax/water emulsion is increased till the maximum value of 99.6% at 0.5 g and time of flotation of 20 min. This increase of the percent removal of the wax can be explained as where soap is acting as soaping agent. The produced foam is increased with increasing the amount of soap and hence the efficiency of flotation process is increased and so the percent of wax removed is increased.

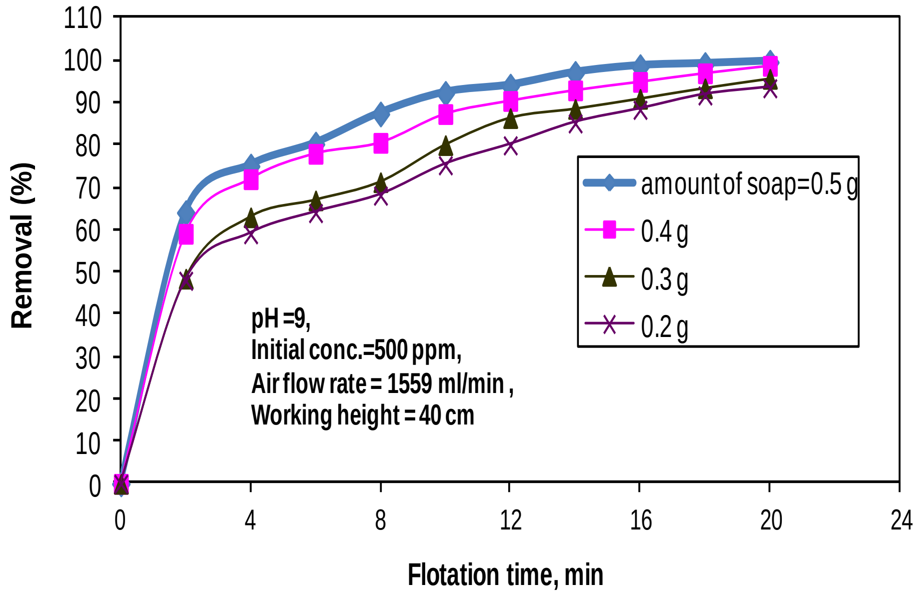

Figure 4. Effect of amount of soap in the scouring process on % removal of wax during flotation.

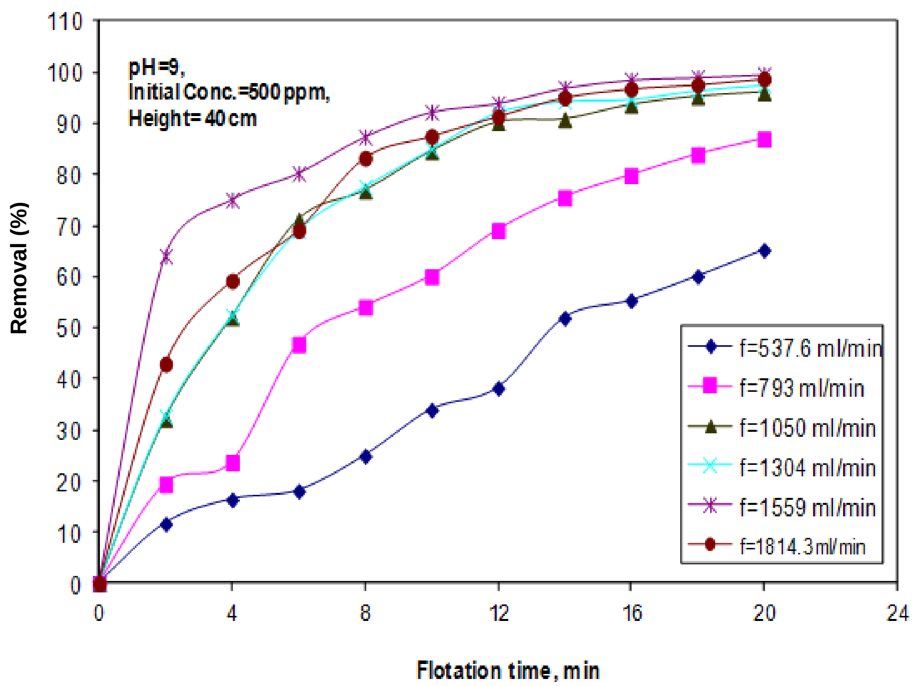

Figure 5. Effect of air flow rate on % removal.

Effect of air flow rate and flotation time

Figure 5 shows the effect of flotation time on the percent of wax removed during the flotation process while Figure 6 shows the effect of air flow rates. Both figures show that with increasing the inlet air flow rate from 538 to 1814 ml/min the percent removal of wax is first increased by increasing the air flow rate till inlet air flow rate

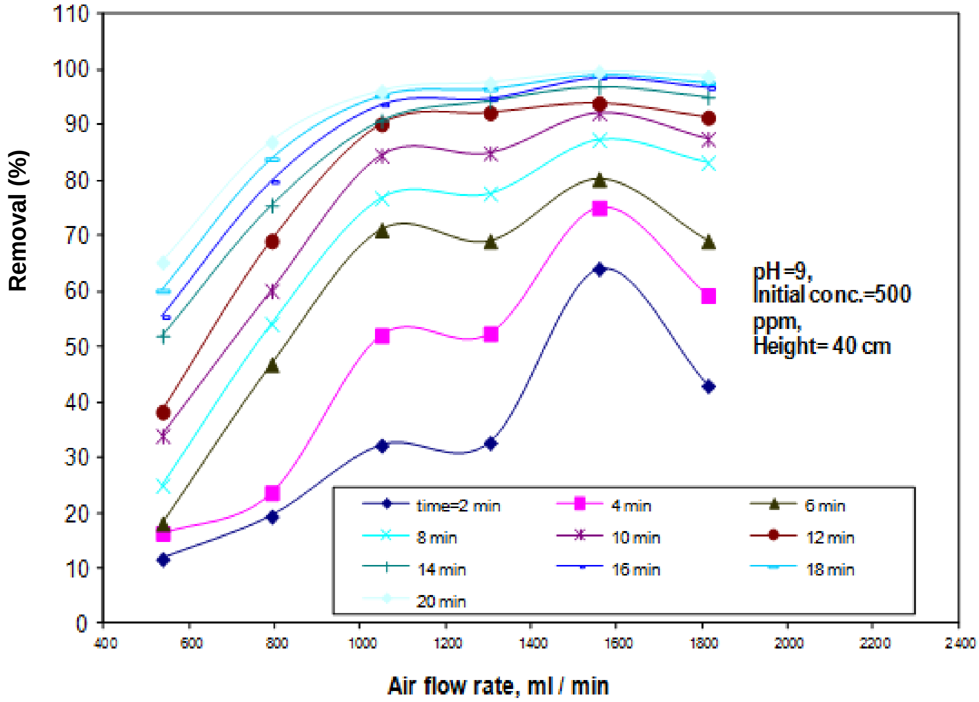

Figure 6. Effect of air flow rate on removal percent.

reaches a value of 1560 ml/min and then it decreases with no any further increase in the inlet flow rate this can be explained as where the efficiency of the flotation process is mainly dependant on the number of air bubbles which carry the oil droplets out of the flotation column. So, with increasing the air flow rate from 538 to 1560 ml/min the number of air bubbles per unit volume is increased and so its ability to carry wax droplets from the W_x/W_a emulsion is increased and thus, the percent of wax removed is increased. On the other hand if the inlet air flow rate is increased more than 1560 ml/min the percent removal of oil is decreased this is not only due to air bubbles slugging, but also due to the formation of eddies which hinder the smooth bubble/droplets rising which was clearly observed visually during the experimental work.

Figure 7 shows the effect of different inlet air flow rates on the wax concentration in the O/W emulsion in the column by using the highest sampling point (at height = 40 cm) and only for 12 min. It was clearly that the highest wax concentration in the column was at the highest sampling point as discussed above. Also it is clear that the wax concentration increased by increasing the air flow rate from 538 to 1560 ml/min and this increase nearly constant after time 10 min for each inlet air flow rate. As it was discussed before that in the flotation process gas bubbles and wax drops have to contact and then attach, but since wax and gas are both less dense than water, they will both rise if present in water. The longer the residence time of the gas bubbles in the flotation tanks, the greater the number of gas bubble-wax droplet collisions (contact efficiency), the greater also the quantity of the wax that ought to be removed (Oh et al., 2009). If the air flow rate is increased up to the optimum value this will give the best number of gas bubbles at the optimum residence time (Jones et al., 1995, Jones and Westmoreland, 1999).

Effect of initial concentration of the wax / water emulsion

Figure 8 shows the relation between the removal percent of wax and time at different initial concentrations of wax/water emulsion. The figure clearly shows that with increasing the initial concentration of wax in the wax water emulsion the removal percent of wax is high. The decrease for 500 ppm initial concentration than that for 250 ppm is somewhat undetectable. This means that the initial concentration of wax/water emulsion do not affect the process up to 500 ppm.

When the concentration of wax in W_x/W_a emulsion is 250 ppm and the air flow rate is 1560 ml/min the produced bubbles has the ability to remove most of the wax droplets present in the wax/water emulsion and when the oil concentration is increased from 250 to 500 ppm and the inlet air flow rate is still 1560 ml/min appear to the produced air bubbles have the ability to remove the

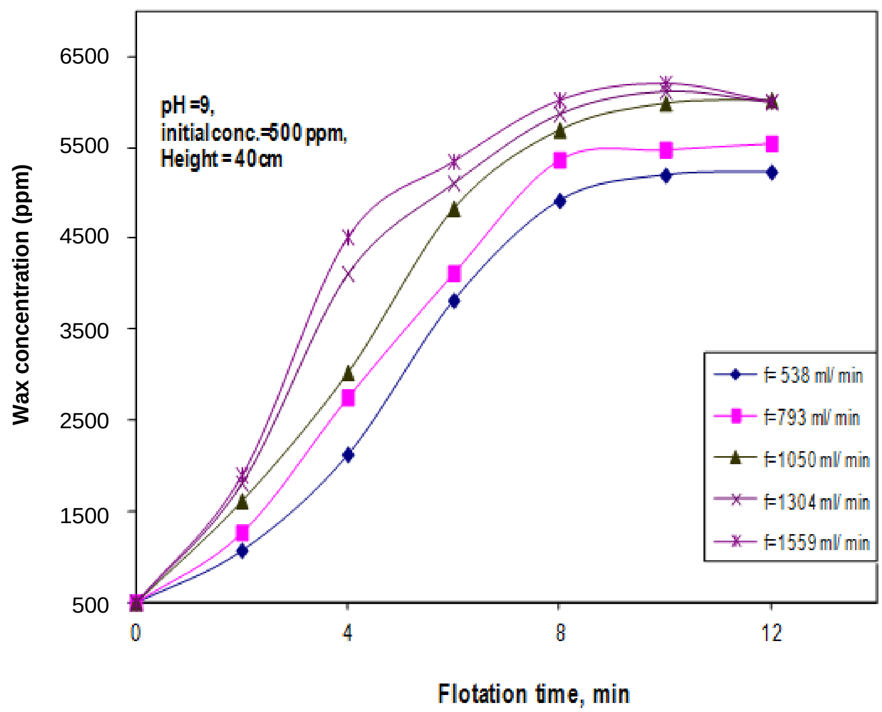

Figure 7. Effect of air flow rate at the heighest sampling point on wax concentration.

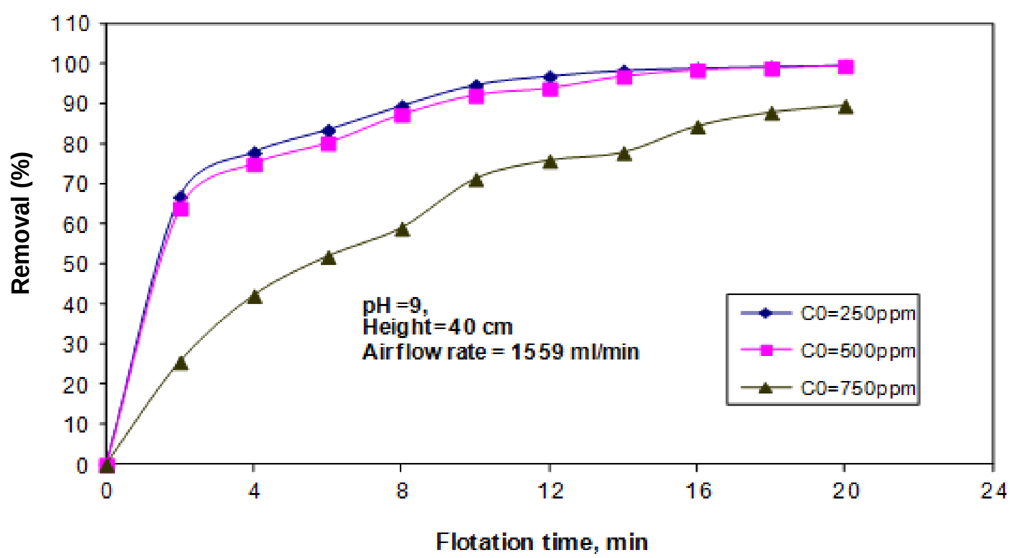

Figure 8. Effect of initial concentration of wax on % removal.

increased amount of wax droplets that result from increasing the wax percent in the wax/W emulsion but when the wax concentration in the W_x/W_a emulsion is increased from 500 to 750 ppm at the same inlet air flow rate of 1560 ml/min, it is noticed that the percent removal of wax is dramatically decreased and this can be attributed to that the number of produced bubbles are not enough to carry all the wax droplets.

If the wax concentration in W_x/W_a emulsion is increased to such a limit that the diameter of wax droplet is more than 200 µm, a primary separator must precede the flotation unit. This is because the gas bubbles cannot

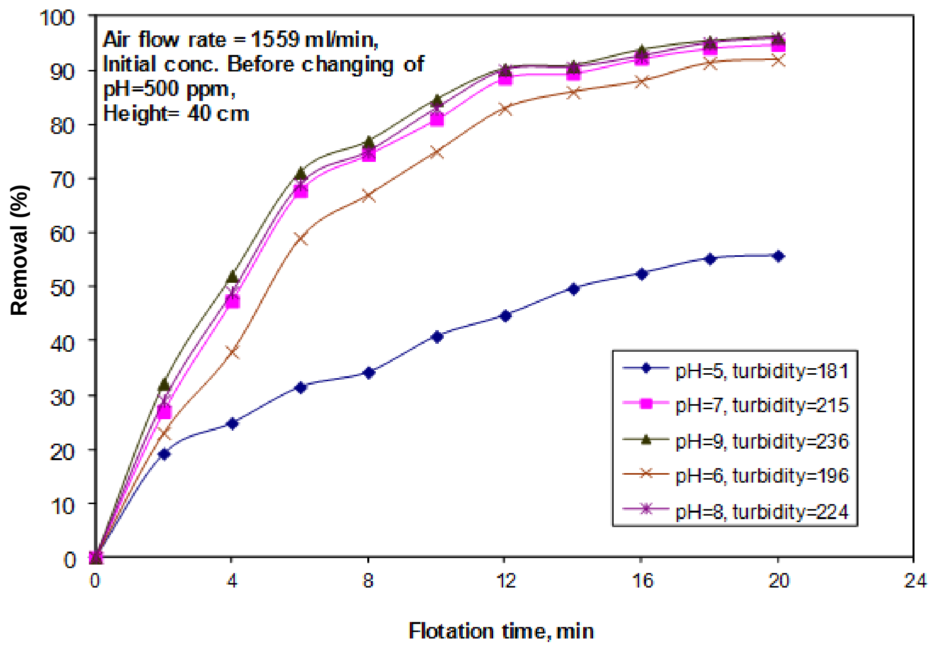

Figure 9. Effect of pH on % removal.

carry such wax droplets so that gas flotation cannot work effectively. Arnold and Stewart (1998) found that when the oil concentration exceeds 1000 mg/L with droplets larger than 200 µm in diameter, a primary separator must precede any flotation unit. This is because the gas bubbles cannot float such large oil droplets, so that gas flotation work effectively. Xuq and Chiang (1999) implied that the oil particle flotation differs from solid particle flotation in that oil–particle attachment may play an important role as bubble–particle attachment at high concentration.

Effect of pH values of the emulsion

Figure 9 shows the relation between the percent removal of wax at different values of pH of the wax/water emulsion at the fixed conditions of airflow rate, initial concentration and height of the batch charge. It is clear that the removal percent of wax from the emulsion increased with increasing pH, taking into consideration that the percent removal of wax is calculated with respect to the equivalent turbidity of the oil/water emulsion at the specified pH.

If the used process for wool scouring is the saponification and emulsification of fatty acid, the process occurs by the use of sodium, triethanolamine soaps by addition of an alkali and a synthetic detergent. The scouring solution penetrates inside the fabric structure allowing for penetration of the impurities at the same time. The alkali contained in the wetting liquor neutralizes free fatty acids on the fabric and forms soaps. Most fatty substances contaminated with the fabric are thus emulsified and eliminated as emulsion (Toro et al., 2012).

The addition of acid decreasing pH value of the wax water emulsion from 9 to 5 separates fatty acids from their soap. This process is commonly used in treating the wax/water emulsion produced from the scouring process (acid cracking) and this is clearly shown from the data where the turbidity of the W_x/W_a emulsion is decreased with decreasing the pH value of the wax water emulsion. Further removal of the wax from the resultant emulsion decrease the efficiency of the flotation processes with decreasing the pH value and this mainly due to the acid cracking. The soaps are dissociated and so the foaming agent which increases the efficiency of the flotation process is decreased. This was noticed visually during the experimental work, which is in agreement with the data in the literature which recommended a flotation after acid cracking to increase the pH value again (Stewart, 1988b).

Effect of working heights of emulsion

Figure 10 shows the relation between the percent removal of wax and time at different working heights of emulsion in the flotation column, while Figure 11 shows the relation between the percent removal of wax and height of wax water emulsion in the flotation column at different flotation times at the fixed conditions of initial concentration, pH and inlet air flow rate. These figures

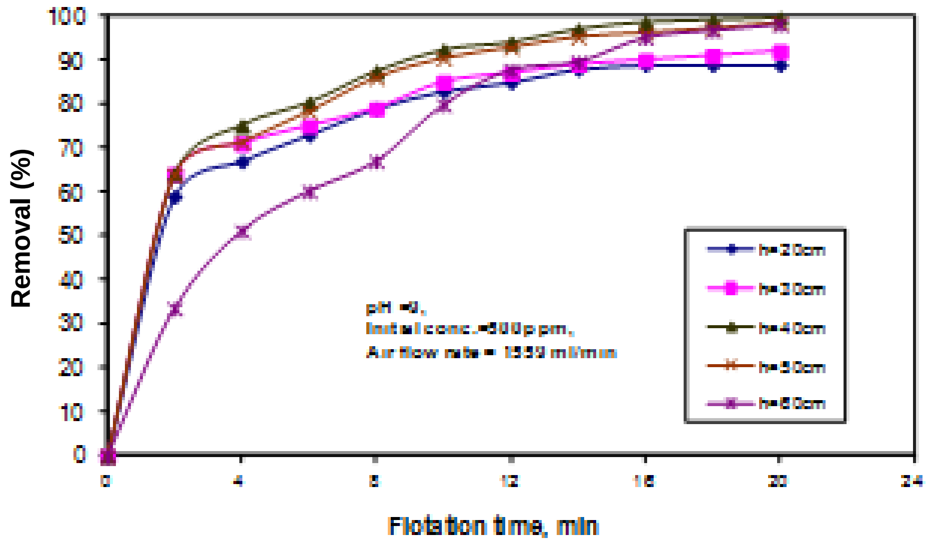

Figure 10. Effect of height of waxy water in the column on % removal.

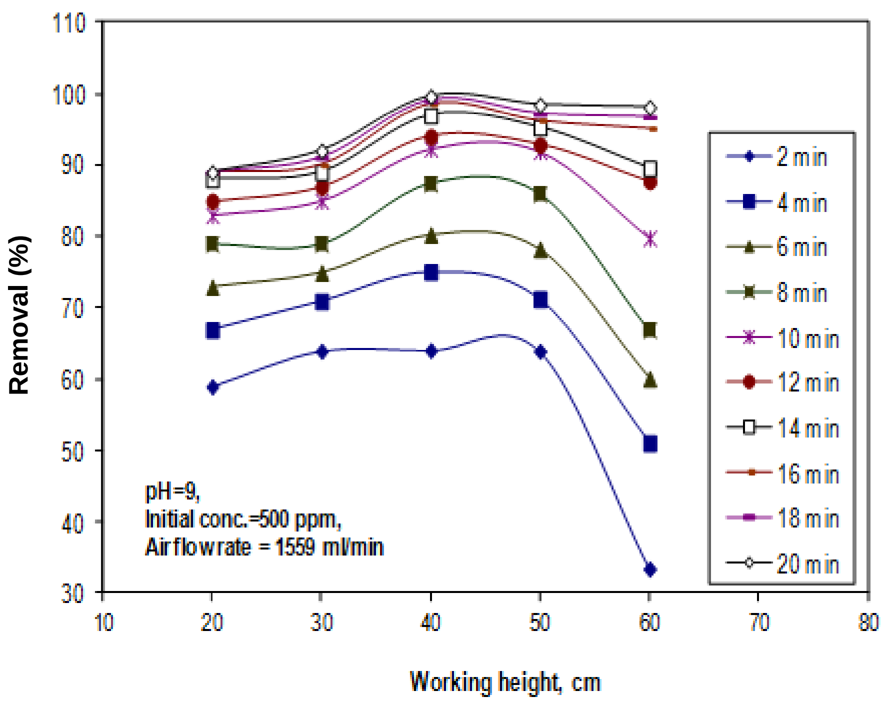

Figure 11. Effect of height of waxy water on % removal.

show that by increasing the working height of the wax water emulsion in the flotation column, the percent removal of wax is increased till 40 cm height then any further increase in the working height decreases the percent removal. By increasing the working height of wax/water emulsion in the flotation column from 20 to 40 cm the percent removal is increased because at the low working height the chance of forming eddies and turbulence is high so that wax does not attached firmly with the air bubbles (diverse flotation process) by increasing the working height from 40 to 60 cm the percent removal is decreased. It seems that the longer

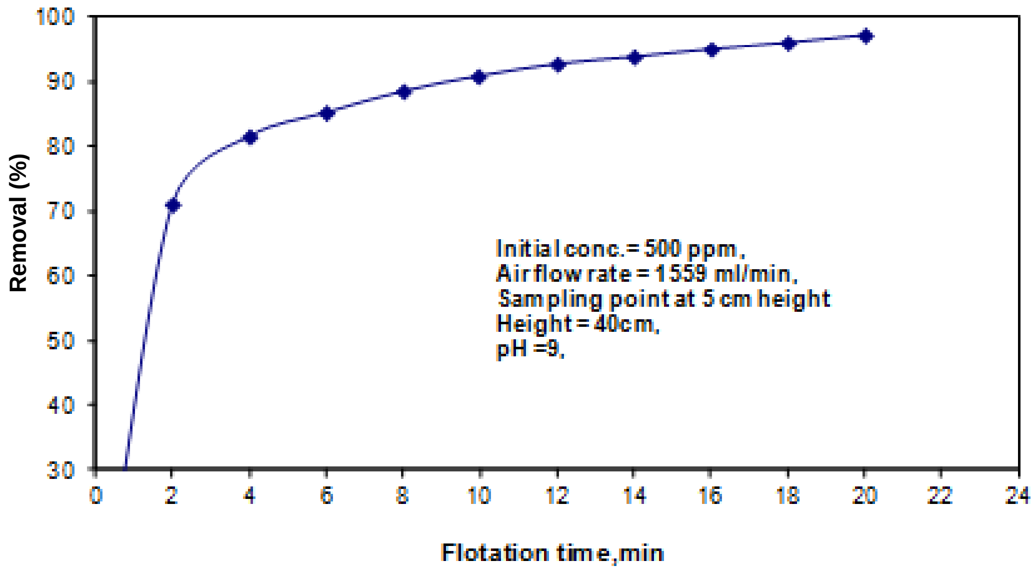

Figure 12. Effect of time of flotation on % recovery.

upward travel of wax droplets makes some separation of wax by loosening its attachment to the air bubbles.

Effect of flotation time on wax recovery

From previous experiments, it is clear that the percent of wax recovery is increased with increasing the flotation time. This increase in percent removal of wax is at high rate in the first period of the flotation process and by time this increase descents. In the first period of flotation where the number of air bubbles per unit volume of the emulsion is high so most of wax droplets are removed rapidly and the removal percent of wax is then high. By further increase the time of flotation the remaining part of wax droplets which is actually smaller than that removed in the first period is also removed but at slower rate.

Figure 12 shows the relation between flotation time and recovery percent at the optimum flotation conditions. The figure shows that the percent of wax recovery is rapidly increased in the first time of flotation, then the recovery rate is decreased. Within the first four minutes nearly about 80% of wax was recovered, while within the following 4 min only 8% recovery was achieved decreasing to only 4 min only 4% recovery is achieved. It is very clear from the economic point of view that the optimum time is 8 min, it can be increased to 10 min for ensuring total gain of wax.

Flotation model

The flotation model is a mathematical description of the separation process and can be used as a benchmarking tool and for optimizing the separation process. Given the type of particle and its size, an engineer can determine the best slurry flow rate, turbulence level and bubble size, so that the particles not only collide with the bubbles but also attach selectively during collision. The particle size determines how quickly and efficiently they collide and attach to the bubbles. Very fine particles collide with the bubbles infrequently and at a much slower rate than large particles, which collide easily but may also detach more readily because of the instability of the bubble/particle union. Among flotation models (Klimpel, 1995; Manqiu, 1998; Polata and Chander, 2000), the most acceptable model is the kinetic model which uses the first order reaction equation as the starting point. It is based on rules of mass trans-port from one phase to another.

In typical first order particle flotation, the collection rate (-dC/ dt) is considered to be proportional to particle concentration. Since the probability of collision among a group of particles is exponentially related to the number of particles, the particle-particle interaction is not important in first order kinetics. However, the interaction among the oil droplets seems to play a significant role in their collection. It can be easily imagined that this interaction increases with the increase in gas velocity and wax concentration. Therefore, if a wax flotation process is expressed in the below form, the kinetic order (n) will decrease with increasing oil concentration as can be summarized from literature data (Chopin et al., 2011; Dominguez et al., 2002; Orbán et al., 2009). The kinetics of an oil flotation process can be expressed by - dC/dt = K Cn, where dC / dt, is the collection rate, C, concentration of wax at any time, K is the rate constant and n, order of the reaction. This is in agreement with the data in the literature (Chipfunhu et al., 2010; Muganda et al., 2010).

It is based on an observation that was made in the earliest experimental kinetic studies of flotation that stated not all particles will be recovered by flotation no matter how much residence time they have in the flotation environment. Work in progress to develop a flotation model to increase the recovery and quality of wax from industrial effluents.

Conclusions

The flotation process proved to be useful for wax recovery from wool scouring effluent in batch flotation processes. The percent of wax recovery was found to increase by increasing the flotation time; the optimum flotation time was 10 min to attain 90% wax recovery. The optimum working height was found to be about eight times the diameter of flotation column. Higher percent recovery is obtained at ph value of 9.

The optimum inlet flow rate was found to be 1560 ml/min. The wax recovery percent was decreased with increasing the initial concentration of wax water emulsion; 500 ppm is the optimum initial concentration for recovery of wax. High wax recovery was obtained by higher soap concentration in the wool scouring liquor. Higher working heights or air flow rates as well as much lower column heights or air flow rates are not sufficient conditions for effective flotation. Moreover, lower pH values and lower soap amounts in the scouring process deteriorate the efficiency of wax recovery process. The kinetics of an oil flotation process can be expressed by first order particle flotation. The rate constant is useful for comparative evaluations of various operating parameters affecting flotation processes. Work in progress to develop a new flotation model to increase the recovery and quality of wax from industrial effluents

ACKNOWLEDGMENT

The authors express their sincere gratitude to Minia university, chemical engineering department for the facilities used in doing the experimental work in the their labs.

REFERENCES

Anna S, Cezary P, Flora P, Christophe B (2012). Fruit cuticular waxes as a source of biologically active triterpenoids, Phytochem. Rev. 11(2-3):263-284.

Arnold KE, Stewart M (1998). 2^{ed},"Surface Production Operation-Design of oil Handling System and Facilities 1. "Gulf publishing Co. Houston Texas (1998).

Athukorala Y, Mazza G (2011). Optimization of Extraction of Wax from Flax Straw by Supercritical Carbon Dioxide. Separation Sci. Technol. 46(2):247-253.

Bateup BO, Christoe JR, Jones FW, Poole AJ, Skourtis C, Westmoreland DJ (1996). "Effluent Management". In-Top Tech.96 Division of Wool Technology, Geelong, Australia.

Bradeley BW (1985). "Flotation Offer Another Water/Oil Separation Alternative", Oil and Gas J. Dec. 1985, pp. 42-46.

Chipfunhu D, Zanin M, Grano SR (2010). The dependency of the critical contact angle for flotation on particle size - modelling the flotation limits for fine particles. Miner. Eng. 24:50-57 (A*, IF=1.022).

Chopin-Doroteo M, Morales-Rueda J, Dibildox-Alvarado E, Charó-Alonso M, Peña-Gil A, Toro-Vazquez J (2011). The Effect of Shearing in the Thermo-mechanical Properties of Candelilla Wax and Candelilla Wax–Tripalmitin Organogels, Food Biophysics. 6(3):359-376.

Christoe JR (1986). "Wastewater Treatment and Disposal". Int. Symposium on Wool Scouring and Worsted Carding New Approaches", CSIRO Division of Textile Industry, Gee long Australia, pp. 24-32.

Christoe JR, Anderson CA, Wood GF (1976). "Biological Destabilization of Wool Scouring Effluents". J. Water Pollut. Control Fed. 48(4):729-735.

Dominguez C, Jover E, Bayona JM, Erra P (2003). "Effect of the Carbon Dioxide Modifier on the Lipid Composition of Wool Wax Extracted From Raw Wool", Analytica Chimica ACTA, 477:23-242.

Dominguez C, Jover E, Bayona JM, Erra P (2002). Effect of the c arbon dioxide modifier on the lipid composition of wool wax extracted from raw wool, Analytica Chimica Acta, 477(2-3):233-242.

Eychene V, Saiz S, Trabelsi F, Recasens F (2001). "Near-critical Solvent Extraction of Wool with Modified Carbon Dioxide-Experimental Results", J. Supercritical Fluid. 21:23-31.

Genon G, Pelosin I, Percivate M (1984). "Anaerobic Digestion of Wool Scouring Wastes". Eur. Cong. Biotechnol. pp. 3-95.

Gibson DM, Morgan WV, Robinson B (1981). "Wool Scouring and Effluent Treatment". Water Sci. Rev. 57:2-32.

Jones FW, Bateup BO, Dixon SR, Gray SR (1995). "Solubility of Wool Wax in Supercritical Carbon Dioxide". J. Critical Fluid.10:10-11.

Jones WF, Westmoreland DJ (1999). "Removal of Wool Wax, Nonylphenol Ethoxylates and Pesticide from Wool Scour Effluent", Wat. Res. 33(8):1775-1780.

Klimpel RR (1995). "The Influence of Frother Structure on Industrial Coal Flotation", High Efficiency Coal Preparation (Kawatra, ed.), Society for Mining, Metallurgy and Exploration, Littleton, CO, pp. 141-151.

Kolattukudy PE (1976). "Chemistry and Biochemistry of Natural Waxes", Elsevier, Amsterdam.

Manqiu Xu (1998). Modified flotation rate constant and selectivity index, Min. Eng. 11(3):271–278.

Max PS, Klaus DT (1980). "Plant Design and Economics for Chemical Engineering", McGraw-Hill Tokyo Japan (1980).

McCracken JR, Chaikin MA (1978). "Physical-Chemical Treatment for Wool Scouring Effluent", Prog. Water Technol, 10(1-2):503-511.

Mercz T, Cord-Ruwisch R (1997). "Treatment of Wool Scouring Effluent Using Anaerobic Biological and Chemical Flocculation", Water Res. 31(1):170-180.

Moldovan Z, Jovere E, Bayona JM (2002). "Systematic Characterization of Long–Chain Aliphatic Ester of Wool Wax by Gas Chromatography-Electron Impact Ionization Mass Spectrometry", J. Chromatography A. 952:193- 204.

Muganda S, Zanin M, Grano SR (2010). Influence of Particle Size and Contact Angle on the Flotation of Chalcopyrite in a Laboratory Batch Flotation Cell. Int. J. Miner. Process. v 98,n(3-4):150-162 (A*, IF=1.017).

Nicholas DS, Byeseda J (1980). "Oil/water Separation by Induced Air Flotation", Petroleum Eng. J. pp. 579-590.

Oh K, Gandhi K, Magda J, Deo MD (2009). Yield Stress of Wax Gel using Vane Method. Petroleum Sci. Technol. 27(17):2063-2073. Taylor and Francis Ltd.

Orbán N, Olivér KI, Drávucz M, Kiss A (2009). LC-MS method development to evaluate major triterpenes in skins and cuticular waxes of grape berries. Int. J. Food Sci. Technol. 44(4):869-873.

Polata M, Chander IS (2000). First-order flotation kinetics models and

methods for estimation of the true distribution of flotation rate constants. Int. J. Min. Process. 58(1–4):145–166.
Poole AJ (2004). “Treatment of Biorefractory Organic Compound in Wool Scour Effluent by Hydroxyl Radical Oxidation”, Water Res. 38:3458-3464.
Poole AJ, Cord-Ruwisch R (2004). “Treatment of Strong flow Wool Scouring Effluent by Biological Emulsion Destabilization”. Water Res. 38:1419-1426.
Poole AJ, Cord-Ruwisch R, Jones FW (1999). “Biological Treatment of Chemically Flocculated Agro-Industrial Waste from the Wool Scouring Industry by an Aerobic Processes without Sludge Recycle”. Water Res. 33(9):1981-1988.
Rajinder P, Masliyan J (1983). “Oil Recovery From Oil in Water Emulsion Using a Flotation Column”. Canadian J. Chem. Eng. 68(6):959-967.
Rippon JA (1992). in D.M. Lewis (ed.) “Wool Dyeing, Society of Dyers and Colorists”,, Bradford,, Chapter 1, (1992).
Rubio J, Souza A, Smith RW (2002). “Overview of Flotation as a Wastewater Treatment Technique”, 15(3):139-155.
Stewart RG (1988a). “Effluent Treatment: Nature of Wool Scouring Wastes”, In Wool Scouring and Allied Technology, Wool Research Organization of New Zealand (Inc). P. 171.
Stewart RG (1988b). “Wool scouring and Allied Technology”, 3rded. NewZealand Christchurch: Wool Research Organization (1988).
Toro-Vazquez J, Morales-Rueda J, Mallia V, Weiss R (2012). Relationship Between Molecular Structure and Thermo-mechanical Properties of Candelilla Wax and Amides Derived from (R)-12-Hydroxystearic Acid as Gelators of Safflower Oil, Food Biophysics 04/2012; 5(3):193-202.
Tsubouchi M, Yamasaki N, Yanagisawa K (1985). “Two–Phase Titration of Poly(oxyethylene) Nonionic Surfactants with Ttrakis (4-flourophenyl)borate”. Anal. Chem. 57:783-774.
Van Ham NJ, Behile LA, Svreck WY (1983). “The Effect of Air Distribution on the Induced Air Flotation of Fine Oil in Water Emulsions”, Canadian J. Chem. Eng. 61:514-547.
Xuq G, Chiang S (1999). “A novel Flotation Column for Oily Water Cleanup”, Separation Purification Technol. 16(3):193-203.

academicJournals

Vol. 8(41), pp. 1966-1974, 9 November, 2013
DOI: 10.5897/IJPS2013.4033
ISSN 1992 - 1950 © 2013 Academic Journals
http://www.academicjournals.org/IJPS

International Journal of Physical Sciences

Full Length Research Paper

Optimal lead-lag controller designing for reduction of load current total harmonic disturtion and hanmonic with voltage control using honey bee mating optimization (HBMO)

Hamdi Abdi[1] and Ramtin Rasoulinezhad[2]*

[1]Electrical Engineering Department, Faculty of Engineering, Razi University, Kermanshah, Iran.
[2]Department of Electrical Engineering, Science and Research Branch, Islamic Azad University, Kermanshah, Iran.

Accepted 22 October, 2013

Increase in world demand load has resulted in new distributed generation (DG) that has entered into the power system. One of the most renewable energies is fuel cell, which is connected to power system using a power electronics interface in microgrid or standalone condition. The highest problem of this switching interface based DGs is the power quality (PQ) and harmonics of currents. Also, the voltage of the DGs should be controlled in islanding condition. In this paper, we present a Lead-Lag optimal controller for controlling one of the most important types of fuel cell, namely proton exchange membrane fuel cell (PEMFC) in islanding mode operation for reducing PQ problems and voltage control. At first, the introduction and implementation of the PEMFC is present and next, during system load variations the proposed controller is designed. The controller should be designed against the demand load variations of fuel cell. Here, the lead-lag controller is used when its coefficients are optimized based on honey bee mating optimization (HBMO). In order to use this algorithm, at first, the problem is written as an optimization problem which includes the objective function and constraints, and then to achieve the most desirable controller, HBMO algorithm is applied to solve the problem. Simulation results are done for various loads in time domain, and the results show the efficiency of the proposed controller in contrast to the previous controllers.

Key words: Power system, fuel cell.

INTRODUCTION

Rising of fossil fuel cost and their probable depletion, air pollution, global warming phenomenon and severe environmental problems that caused distributed energy sources have gained the attention of many nations in producing electricity. High efficiency and very low emissions can be satisfied in fuel cell-based power generation systems. Moreover, fuel cells have a superior dynamic response, good stability and low noise. Proton exchange membrane fuel cell (PEMFC) can be a great alternative for power generating sources in the coming years, especially in the automotive, distributed power generation, and portable electronic applications (Alireza and Alireza, 2011).

PEMFC is composed of cathode, anode and electrolyte between the anode and cathode. Hydrogen gas (H_2), which is obtained from methanol (CH_3OH), is inserted into the end of the anode blade and oxygen or air at the end of the positive electrode of the cell (cathode) (Mo

*Corresponding author. E-mail: chibueze.nnaji@unn.edu.ng, Tel: +234(0)8030967563.

Zhigun et al., 2005).

In the previous literature, various models have been developed for the PEMFC system dynamic modeling, analysis, control and operation. A type of fuzzy controller that controls the fuel cell output voltage is considered by Mo Zhigun et al. (2005). BP and RBF networks control strategy for voltage and current control of the fuel cell is used by Yanjun et al. (2006). The development of a computer model for simulating the transient operation of a tubular solid oxide fuel cell (SOFC) is described by David et al. (1999). The power quality in an FC-based on power system is affected by the harmonic contents of the current waveform injected to the load / grid by the inverter and also by the harmonic currents produced by the non linear loads connected to the system (Tanrioven and Alam, 2006). In addition, the harmonics injected by the inverter would increase in the FC connected to a distribution generation DC bus with devices such as photovoltaic and wind turbines. The electrochemical and thermal parts of the model were developed and verified separately before they were combined to form the transient model. The model includes the electrochemical, thermal, and mass flow elements that affect SOFC electrical output. A nonlinear lumped-parameter mathematical model of direct reforming carbonate fuel cell stack is considered by Michael et al. (2001). Analytical detailed active and reactive power output of a stand-alone PEM fuel cell power plant (FCPP) is controlled (El-Sharkh et al., 2004). The validity of the analysis in this paper is verified when the model is used to predict the response step changes in the active load and reactive power demand and actual active and reactive load profile.

The ripple current propagation path is analyzed by Changrong and Jih-Sheng (2007), who derived its linear AC model. Equivalent circuit model and ripple current reduction with passive energy storage and advanced active control technique are then proposed to incorporate a current control loop in the DC–DC converter, which is used for this goal. A fully integrated modeling approach that lends itself to parallelism is introduced by Abdelkrim et al. (2010). Simulation time reduction with parallel computing is achieved with this modeling. Gemmen (2003) suggested that the ripple current be limited to less than 10%. Passive energy storage compensation method was suggested and tested extensively by Schenck et al. (2005). Active compensation with external bidirectional DC–DC converter method was suggested by Novaes and Barbi (2003) and Monti et al. (2002). These methods require externally added components or circuits and are not preferred.

To produce electrical energy from the fuel cell, it is essential that the output voltage of cell be kept constant for different loads to supply high quality power to the loads. Also the Power Quality (PQ) problems should be solved in islanding mode operation of fuel cell. . In this paper, a simple Lead-Lag controller is proposed for fuel cell voltage control, reducing the current Total Harmonic Distortion (THD) and Current Harmonic (CH) reduction. The proposed controller is design based on HBMO algorithm. In order to achieve the optimal Lead-Lag controller at first, the problem is converted to optimization problem and then is solved by using HBMO algorithm. The main goal of this optimization problem is to regulate the voltage of PEM. The advantages of the proposed control are as follows: 1- controllers are simple, 2- its robustness against load changes, 3- has the desired control features, 4- has fast transient response and 5- has zero steady error.

Dynamic model of the fuel cell

Firstly, to study the dynamic behavior of the fuel cell, the scheme, structure and modeling of the fuel cell should be done. Figure 1 shows the schematic model of the fuel cell system proposed as voltage controller that is applied in this paper. The mass of the anode and cathode in the figure is considered as a sole compression of anode and cathode (Noradin et al., 2012). The dynamic model of the PEMFC system is based on Akbar et al. (2012). The equal output voltage of the PEMFC system is extracted by deducing the voltage drops from the regressive voltage. Equation (1) expresses how to calculate the fuel cell output voltage (Noradin et al., 2012).

$$V_s = n(E_{reversable} - V_{act} - V_{ohmic} - V_{con}) \quad (1)$$

Where, V_s is the accumulated fuel cell outandut voltage in volts, n is the existing cells in the accumulated fuel cell, V_{act} is the voltage drop resulting from anode and cathode activity in volts, V_{ohmic} is the ohmic voltage drop in volts, which is a certain amount of resistance in the transfer of electrons and protons in the electrolyte between the anode and cathode. V_{con} results from the mass transfer of oxygen and hydrogen. $E_{reversable}$ in equation (1) is calculated through the following Equations (1) and (10).

$$E_{reversable} = 1.229 - 0.85\times10^{-3}(T - 298.15) + 4.3085\times T\times[\ln(PH_2 + 0.5\ln(PO_2)] \quad (2)$$

Where, T is the cell temperature in Kelvins, PH_2, PO_2 are effective partial pressure (atm) of hydrogen and oxygen gases respectively that can be calculated by the following equation,

$$PO_2 = P_c - P_{H_2o}^{sat} - P_{N_2}^{channel}\exp\left(\frac{0.291\left(\frac{i}{A}\right)}{T^{0.932}}\right) \quad (3)$$

$$PH_2 = 0.5P_{H_2o}^{sat}\left(\frac{1}{\exp\left(\frac{1.635\times\left(\frac{i}{A}\right)}{T^{1.334}}\right)\cdot\left(\frac{P_{H_2o}^{sat}}{P_a}\right)} - 1\right) \quad (4)$$

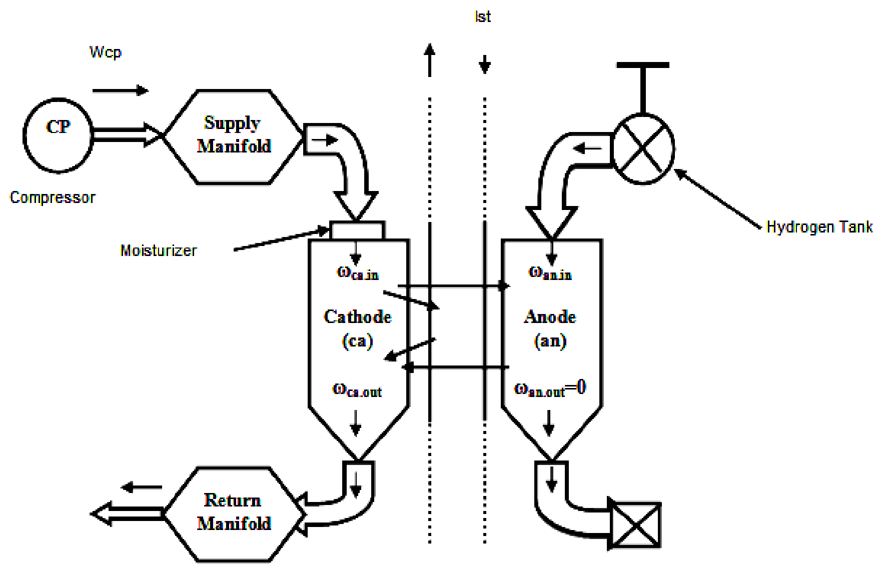

Figure 1. Schematic diagram of fuel cell.

Where, P_a and P_c are the anode and cathode inlet pressure in atmospheres, A is the effective electrode area in Cm^2, i is the current of each cell in amperes, $P_{H_2o}^{sat}$ is the amount of saturated steam pressure whose value depends on the fuel cell. $P_{N_2}^{channel}$ is the partial pressure of N_2 in the cathode gas flow channels in atmospheres which can be calculated by the following equation,

$$P_{N_2}^{channel} = \frac{0.79}{0.21} PO_2 \quad (5)$$

All the amounts used in this article are the same with data available in the work of Noradin Ghadimi, (2012).

Honey bee mating optimization

Honey bee is a social insect that can survive only as a member of a community or a colony. The colony inhabits an enclosed cavity. A colony of honey bees consist of a queen, several hundred drones, 30,000 to 80,000 workers and broods during the active season. A colony of bees is a large family of bees living in one bee-hive. The queen is the most important member of the hive because she is the one that keeps the hive going by producing new queen and worker bees (Taher, 2011). Drones' role is to mate with the queen. Tasks of worker bees are several such as: rearing brood, tending the queen and drones, cleaning, regulating temperature, gathering nectar, pollen, water, etc. Broods arise either from fertilized (represent queen or worker) or unfertilized (represent drones) eggs. The HBMO Algorithm is the combination of several different methods corresponded to a different phase of the mating process of the queen. In the marriage process, the queens mate during their mating flights far from the nest. A mating flight starts with a dance performed by the queen who then starts a mating flight during which the drones follow the queen and mate with her in the air. In each mating, sperm reaches the spermatheca and accumulates there to form the genetic pool of the colony. The queen's size of spermatheca number equals to the maximum number of matings of the queen in a single mating flight is determined. When the queen mates successfully, the genotype of the drone is stored. At the start of the flight, the queen is initialized with some energy content and returns to her nest when her energy is within some threshold of zero or when her spermatheca is full. In developing the algorithm, the functionality of workers is restricted to brood care, and therefore, each worker may be represented as a heuristic which acts to improve and/or take care of a set of broods. A drone mates with a queen probabilistically using an annealing function (Yannis et al., 2011):

$$P_{rob}(Q,D) = e^{-\frac{\Delta(f)}{s(t)}} \quad (6)$$

Where Prob (Q, D) is the probability of adding the sperm of drone D to the spermatheca of queen Q (that is, the probability of a successful mating); Δ (f) is the absolute difference between the fitness of D (that is, f (D)) and the fitness of Q (that is, f (Q)); and S (t) is the speed of the queen at time t. It is apparent that this function acts as an annealing function, where the probability of mating is high when both the queen is still in the start of her mating–flight and therefore her speed is high, or when the fitness of the drone is as well as the queen's. After each transition in space, the queen's speed, S(t), and energy E(t) decay using the following equations:

$$S(t+1) = \alpha \times s(t)(2) \quad (7)$$

$$E(t+1) = E(t) - \gamma \quad (8)$$

Where α is a factor and γ is the amount of energy reduction after each transition. Also, Algorithm and computational flowchart of HBMO method to optimize the PEM controller parameters is presented in Figures 2 and 4. Thus, HBMO algorithm may be constructed in the following five main stages:

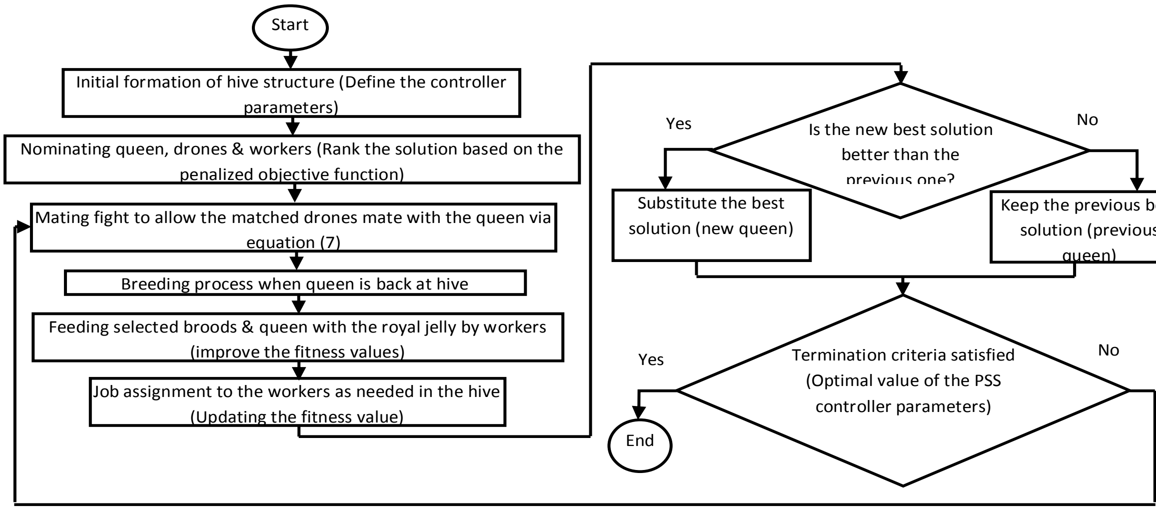

Figure 2. Algorithm and computational flowchart of HBMO.

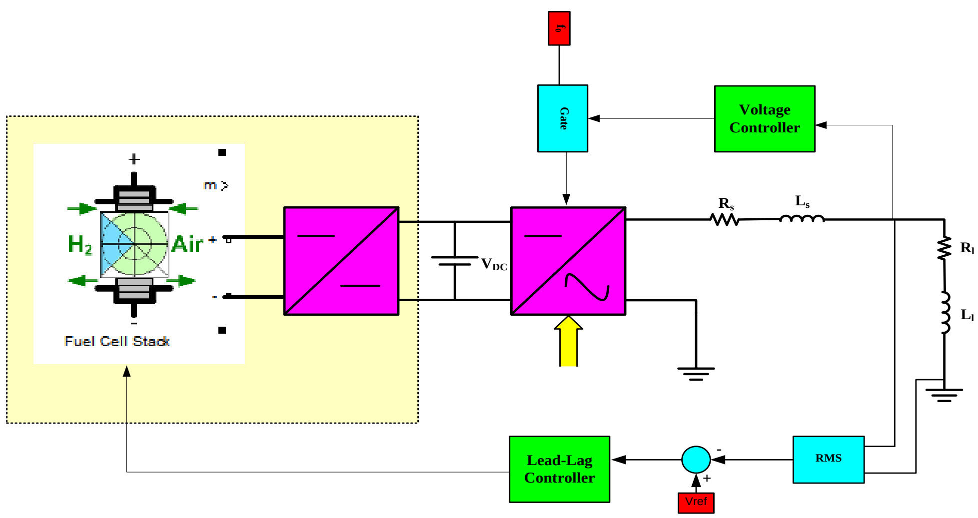

Figure 3. Single line diagram of DG, local load, controller and grid.

(i) The algorithm starts with the mating–flight, where a queen (best solution) selects drones probabilistically to form the spermatheca (list of drones). A drone is then selected from the list at random for the creation of broods.
(ii) Creation of new broods by crossover ring the drones' genotypes with the queen's.
(iii) Use of workers (heuristics) to conduct local searches on broods (trial solutions).
(iv) An adaptation of workers' fitness based on the amount of improvement achieved on broods.
(v) Replacement of weaker queens by fitter broods.

Study system description

Schematic diagram of an electronically coupled PEMFC, DG unit is depicted in Figure 3. In this figure, DG unit is connected to load via a low pass filter R_t, L_t and VSC. Parameters of the system are listed in Table 1.

Table 1. Parameters of DG, local load and grid.

Parameter	Value
R	3.8 Ω
Rt	0.075 mΩ
Lt	15 µH
VSC rated power	5 kW
PWM carrier frequency	1,980 HZ
f0	50 HZ
Nominal Load voltage	110 V (rms)

This system should be working in islanding mode. Depending on the load value, voltage of local load may be increased or decreased and even it may approach instability. Although, in the case of rated load, the voltage and the frequency would remain in nominal value.

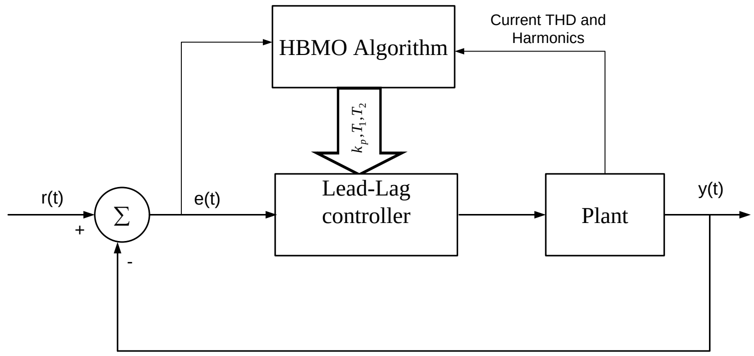

Figure 4. Schematic of the proposed controller designing.

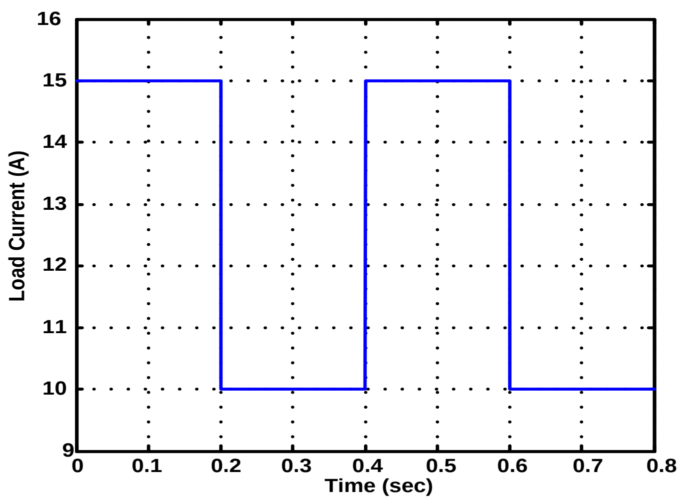

Figure 5. Worst case of load variation of PEMFC.

Also, based on load current, the harmonic current can be produced. Thus, it is necessary for system, different controller appropriate for improving system performance.

Using HBMO to adjust controller parameters

Due to the development of system controllers, the conventional controllers are used widely in power system applications. Applying conventional controllers is simple against the new controllers of power systems (Akbar et al., 2012). The Lead-Lag controllers are widely used in most cases of power system controllers which compensate very well. One of the highest benefits of these controllers is the easily implemention in analog and digital systems. If these controllers are designed optimally, indubitable they become one of the most implemented controllers in modern systems. This paper introduces a new optimal Lead-Lag controller, which is used by HBMO algorithm for designing the controller of proton exchange membrane fuel cell in order to control OD voltage and improve the PQ. The overall controller schematic is shown in Figure 4.

Lead-Lag general controller is expressed in Equation (9) in which the controller k_p, T_1, T_2 parameters should be optimized using the proposed algorithm. In the load variations, it is obvious that the transient mode of the PEMFC system depends on the controller parameters. The conventional controller designing method is not viable to be implemented because this system is an absolute nonlinear. So these methods would have no efficient performance in the system.

$$G_c(s) = k_p \frac{1+sT_1}{1+sT_2} \qquad (9)$$

In order to design an optimal controller using HBMO for the fuel cell from the load current curve, we consider the worst condition for load design controllers for these conditions. Figure 5 depicts the worst condition for a load current in the system for voltage equal to 200V. At first, the problem should be written as an optimization problem and then by applying the proposed optimization method, the best Lead-Lag controller is achieved. Selecting objective function is the most important part of this optimization problem. This is because choosing different objective functions may completely change the particle's variation state. In optimization problem, we considered the voltage error signal, total harmonic distortion of current and 3rd harmonic of current in order to achieve the best controller.

$$J = \int_{tstart}^{tsim} \left[\left| V_{ref} - V_{out} \right| + \left| THD_i \right| + \left| I_h^{3th} \right| \right] dt \qquad (10)$$

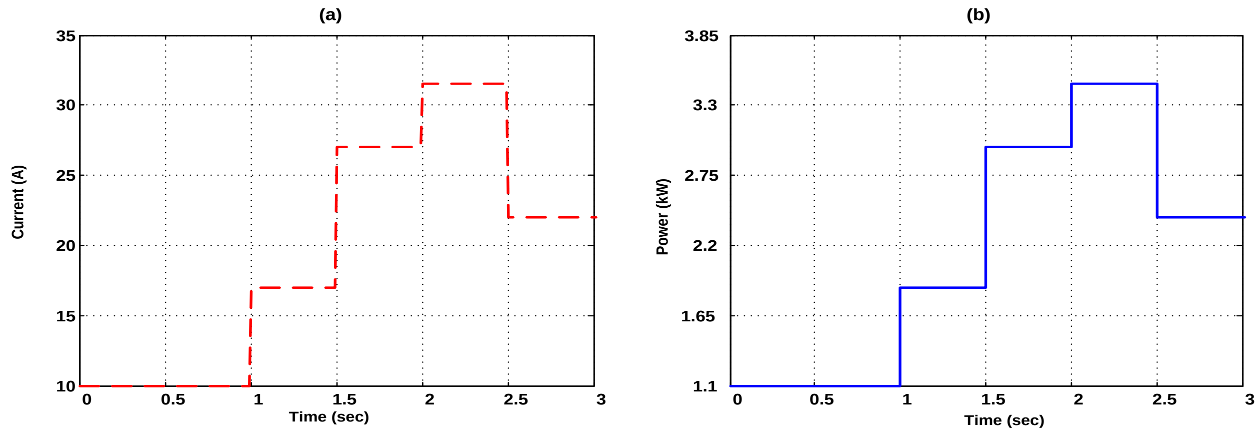

Figure 6. Load variation considering constant voltage for the fuel cell a) current b) demand power.

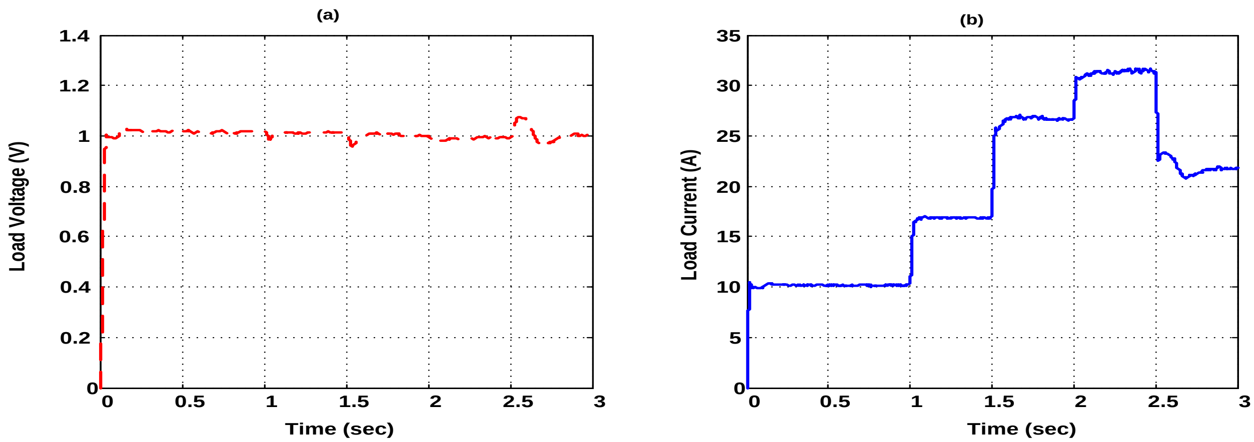

Figure 7. the results of proposed controller for load changing condition a) output voltage and reference voltage b) anode and cathode gas pressure with load current.

Where, *tsim* is the simulation time in which objective function is calculated, V_{out} is the real output voltage and V_{ref} is the reference voltage, THD_i is the current total harmonic distortion and $\left|I_h^{3th}\right|$ is the 3rd current harmonics. We are reminded that when the objective function is a small amount, in this case the answer will be more optimized. Each optimizing problem is optimized under a number of constraints. Problem constraints should be expressed as:

$$\begin{aligned} &Minimize\,J \ subject\ to \\ &k_p^{\min} \le k_p \le k_p^{\max} \\ &T_1^{\min} \le T_1 \le T_1^{\max} \\ &T_2^{\min} \le T_2 \le T_2^{\max} \end{aligned} \qquad (11)$$

Where, T_1, T_2 are in the interval [0.01 2] and k_p in the interval [1 500]. In this problem, the number of particles, the dimension of the particles, and the number of repetitions are selected as 40, 3, 80, respectively. After optimization, results are determined as:

$$k_p = 134.1\ , T_1 = 0.077\, , T_2 = 1.7240 \qquad (12)$$

Simulation results

The load curve variation for fuel cells is considered in order to show good performance of the proposed algorithm. Desired load current is plotted in Figure 6(a) and in Figure 6(b); the amount of fuel cell power demand or load power variation is displayed. Desired load is considered under the constant output voltage, while the current is changing between the range of 10 to 32 amperes and its variations are considered to show the performance of the proposed controller in transient times. Simulation output results obtained from the proposed algorithm which is expressed in Equation (12) are shown in Figures 7, 8 and 9. Figure 7(a) depicts PEMFC's

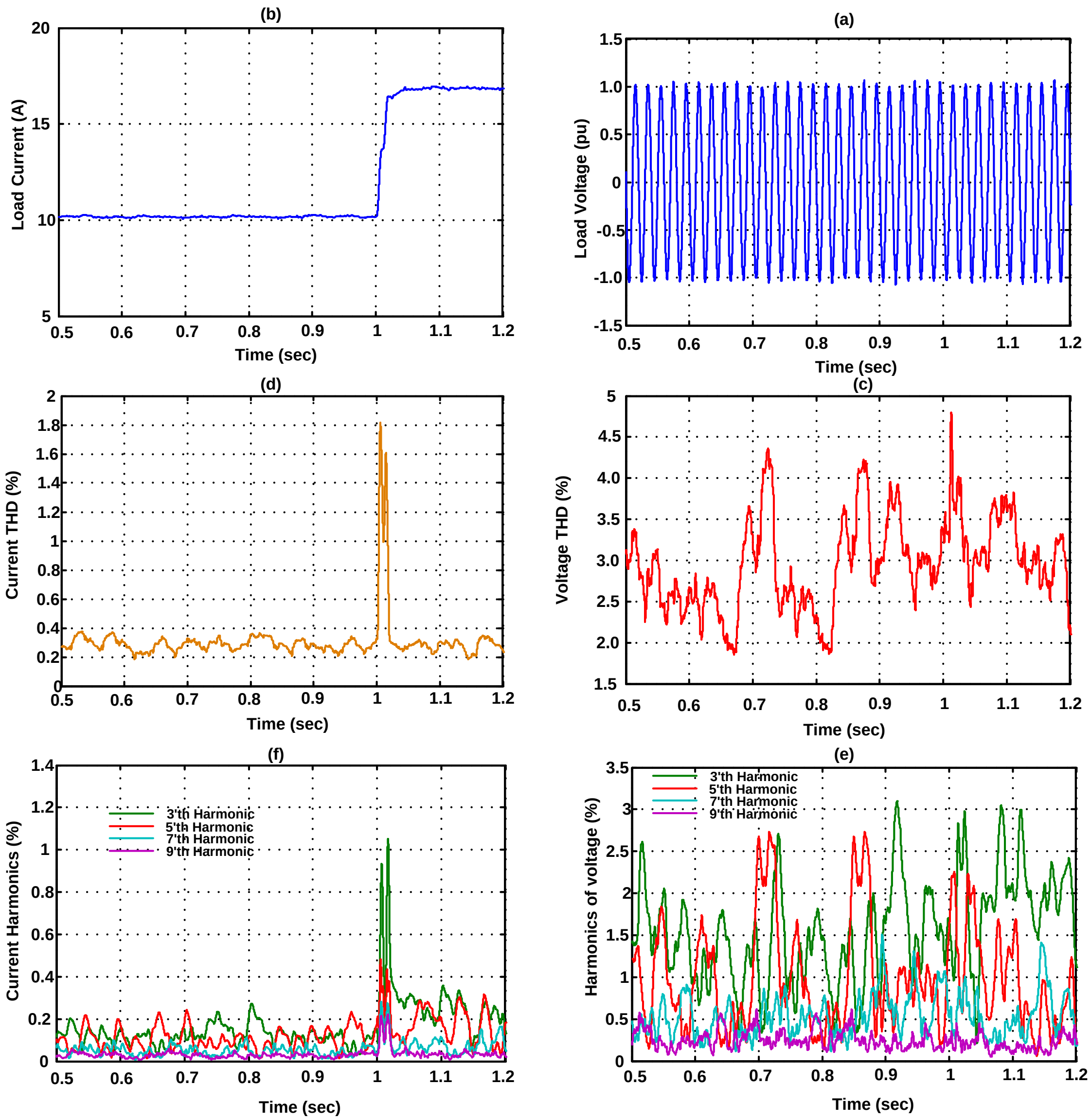

Figure 8. Transient response in load changing using proposed controller a) reducing of demand power b) increasing of demand power.

output voltage which is about 1 pu. Figure 7(b) shows the variation of load current of demand load that reaches the reference current signal. From this Figure, it can be seen that by changing load current, gas pressure in the anode and cathode change quickly to keep stable the output voltage of the fuel cell at 1 pu and this shows good performance of the proposed controller albeit simplicity. Also, according to an output voltage of load and reference voltage, it is obvious that controller response is appropriate and it could follow the reference voltage properly.

In Figure 8(a) and (b), the load voltage and current are plotted in increasing load variation condition, respectively. From the figure, it is obvious that the proposed controller can control the load voltage. Figure 8(c) and (d) show the THD value of voltage and current, respectively. It can be seen that, the THD of the voltage is lesser than 5% and THD of current is lesser than 2%. The harmonics of voltage and currents are plotted in Figure 8(e) and (f), respectively. These results have shown the high efficiency of the proposed algorithm. At t=2.5 s, reducing step in load switching occurrs. Figure 9 depicts the results of the proposed algorithm for this condition. Figure 9(a) and (b) show the load voltage and current in reducing load variation condition, respectively. From the figure, it is obvious that the proposed controller can control the load voltage. The THD value of voltage and current is plotted in Figure 9(c) and (d), respectively. It

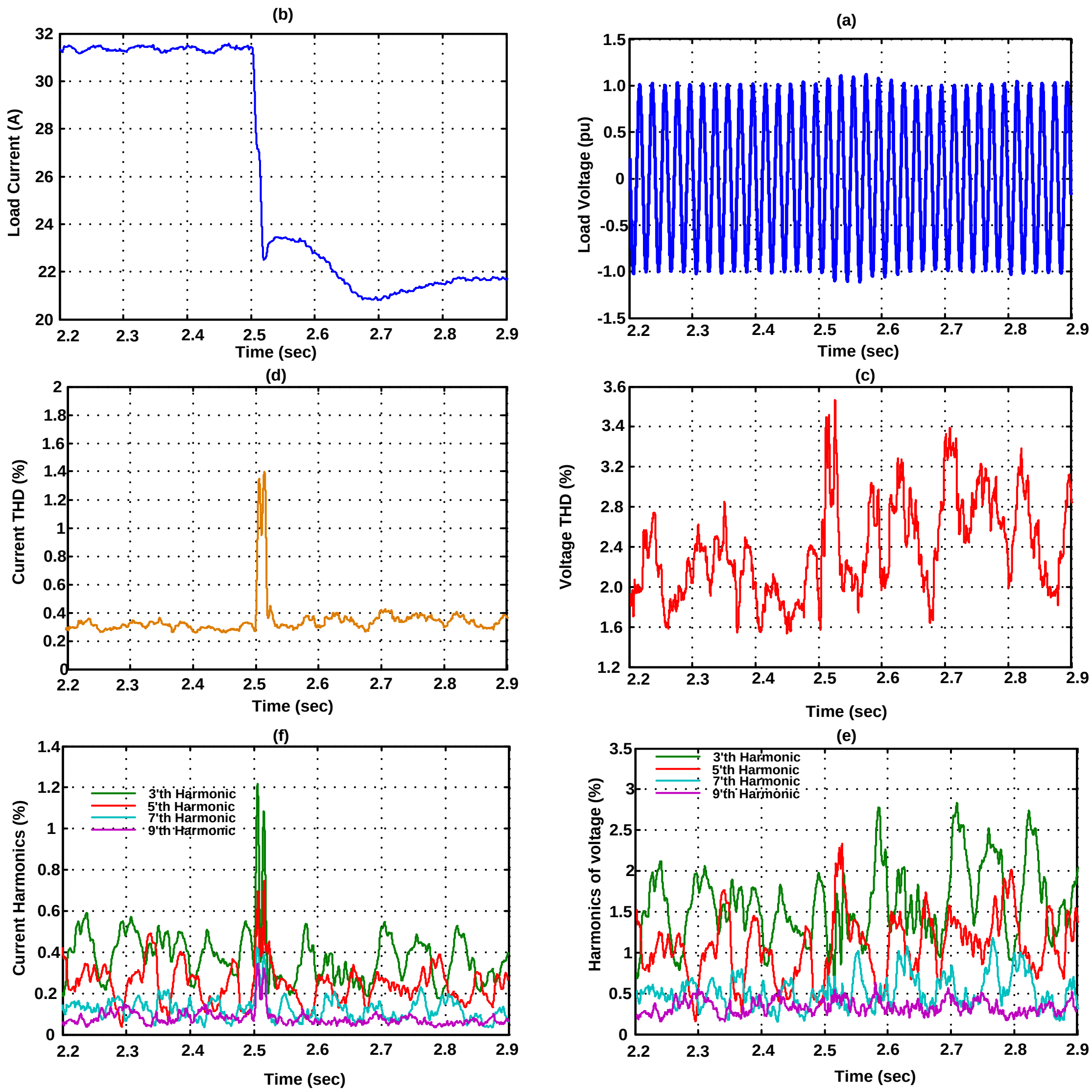

Figure 9. Transient response in applying the disturbance in anode and cathode gas.

can be seen that, the THD of the voltage is lesser than 3.6% and THD of current is lesser than 1.4%. The harmonics of voltage and currents are plotted in Figure 9(e) and (f), respectively. From these results, one can say the proposed controller is an optimal controller for PEMFC system.

CONCLUSION

Optimal controller designing for voltage control and power quality improvement using HBMO based Lead-Lag controller was proposed in this paper. For simplicity, easy implementation, high efficiency features of the Lead-Lag controller, this controller is chosen in this paper. To obviate the problem of the previous controller HBMO algorithm was utilized to design the Lead-Lag controller to have the most optimized state. In solving this problem, the problem was first written in the form of the optimization problem in which its objective function was defined and written in time domain; and then the problem was solved using HBMO algorithm. The objective function contains three parts, namely: voltage error signal, total harmonic distortion of current signal and the 3rd harmonic signal of current. The most optimal mode for gain coefficient and controller zero and pole was determined using the algorithm.

REFERENCES

Abdelkrim S, Jaafar G, Rachid O, Olivier S, El-Sayed H (2010). Modeling and Simulation of PEM Fuel Cell Thermal Behavior on Parallel Computers. IEEE Trans. Energy Conver. 25(3):768-777.

Akbar H, Mehdi M, Ramtin RN, Noradin G (2012). Designing PID Controller for Fuel Cell Voltage Using Evolutionary Programming Algorithms, J. Basic. Appl. Sci. Res. 2(2):1981-1987.

Alireza A, Alireza R (2011). Artificial immune system-based parameter extraction of proton exchange membrane fuel cell. Electrical Power Ener. Syst.33:933–9384.

Changrong L, Jih-Sheng L (2007). Low Frequency Current Ripple Reduction Technique With Active Control in a Fuel Cell Power System With Inverter Load. IEEE Trans. Power Electronics, 22(4):1429.

David J, Hall R, Gerald C (1999). Transient Modeling and Simulation of a Tubular Solid Oxide Fuel Cell, IEEE Trans. Energy Conversion, 14(3):749-753.

El-Sharkh MY, Rahman A, Alam MS, Sakla AA, Byrne PC, Thomas T (2004). Analysis of Active and Reactive Power Control of a Stand-Alone PEM Fuel Cell Power Plant,, IEEE Trans. Power Syst. 19(4):2022-2028.

Gemmen RS (2003). “Analysis for the effect of inverter ripple current on fuel cell operating condition,” J. Fluids Eng. 125(3):576–585.

Michael DL, Kwang YL, Hossein G (2001). An Explicit Dynamic Model for Direct Reforming Carbonate Fuel Cell Stack. IEEE Trans. Energy Conver.16(3):289-295.

Monti A, Santi E, Ponci F, Franzoni D, Patterson D, Barry N (2002). “Fuel cell based domestic power supply-a student project,” in Proc. IEEE Power Electronics Specialists Conf., Cairns, Australia, Jun. 2002, pp. 315–320.

Noradin G (2012). Genetically tuning of lead-lag controller in order to control of fuel cell voltage, Sci. Res. Essays 7(43):3695-3701.

Noradin G, Mohammad M, Rasoul G (2012). Adjusting Parameters of Lead Lag Controller Using Simulated Annealing to Control Fuel Cell Voltage, Res. J. Infor.Technol. 4(1):23-26.

Novaes YR, Barbi I (2003). “Low frequency ripple current elimination in fuel cell systems,” in Proc. Fuel Seminar Special Session on Fuel Cell Power Conditioning, Miami, FL, 2003, pp. 21–27.

Schenck M, Stanton K, Lai JS (2005). “Fuel cell and power conditioning system interactions,” in Proc. IEEE Applied Power Electronics Conf., Austin, TX, Mar. 2005, pp. 114–120.

Taher N (2011). “An efficient multi-objective HBMO algorithm for distribution feeder reconfiguration,” Expert Syst. Applications, 38(3):2878–2887.

Tanrioven M, Alam MS (2006). “Modeling, Control, and Power Quality Evaluation of a PEM Fuel Cell –Based Power Supply System for Residential Use.” IEEE Trans. Industry Applications, 42:6. November/December 2006.

Yanjun L, Houjun W, Zhijian D (2006). “Using Artificial Neural Network to Control the Temperature of Fuel Cell”IEEE Conference 2006, pp. 2159-2162.

Yannis M, Magdalene M, Georgios D (2011). “Honey bees mating optimization algorithm for the Euclidean traveling salesman problem,” Infor. Sci. 181(20):4684–4698.

Zhigun M, Xinjian Z, Guangyi C (2005). “Design and Simulation of Fuzzy Controller for PEMFCs” IEEE Conference. 2005, pp. 220-224.


International Journal of
Physical Sciences
OPEN ACCESS